Available online www.ejaet.com

European Journal of Advances in Engineering and Technology, 2024, 11(10):14-45

Research Article ISSN: 2394 - 658X

The Deadliest and Costliest Typhoon in the Philippines: Two-Dimensional Wind and Pressure Fields Generation for Super Typhoon Haiyan (Yolanda) in 2013

Md. Akhtaruzzaman Sarker (PhD)

Technical Director, Royal HaskoningDHV, Westpoint, Peterborough Business Park,
Lynch Wood, Peterborough PE2 6FZ, United Kingdom.
E-mail: zaman.sarker@rhdhv.com

ABSTRACT

Significant loss of life and damage to properties, marine facilities and ecosystems are caused by typhoons (also known as cyclones or hurricanes). Climate change is likely to worsen the problem. Typhoon modelling results are used for deriving robust design conditions for coastal and marine structures and facilities. These are also used for emergency planning and decision-making to estimate potential loss of life, damage to properties and marine facilities and to develop rescue and mitigation measures and plan clean-up operations. Typhoon Haiyan (2013), known in the Philippines as Super Typhoon Yolanda, was the deadliest and costliest typhoon in the Philippines and, therefore, this paper has focused to this event. Raw data (such as track, wind speed, central pressure, and radius of maximum wind speed) were obtained from IBTrACS. Two-dimensional wind and pressure fields along the entire track were then generated using the Cyclone Wind Generation Tool developed by DHI. Two-dimensional wind and pressure fields at selected locations along the track are presented in this paper. Time-series wind speed and pressure over the entire passage of the typhoon are also provided at these selected locations. These wind and pressure fields are useful for numerical modelling of waves and surge. Structural design considerations and typhoon risk reduction measures are also described in this paper. The methodology described in this paper for generating wind and pressure fields from Typhoon Haiyan could also be applied for other typhoons around the world.

Keywords: Natural Hazards, Cyclones, Hurricanes, Typhoons, Typhoon Haiyan, Port Development, Royal HaskoningDHV.

INTRODUCTION

Formation of Typhoons

Tropical cyclones (also known as hurricanes or typhoons) are associated with warm and moist air and hence they form only over warm ocean waters near the equator (within latitude 30° north and south). They need some favourable conditions to form such as:

a) Warm sea surface temperature
b) Large convective instability
c) Low level positive vorticity
d) Weak vertical wind shear of horizontal wind
e) Coriolis force

Warm ocean waters of at least 27°C throughout a depth of about 50m from sea surface is required for cyclone formation. The warm and moist air rises causing an area of lower pressure beneath. Cooler air moves into the lower pressure area and becomes warm and moist and rises too. When the warm and moist air rises, it cools down and forms clouds. The entire system of clouds and winds spins and grows and is fed by ocean’s heat and evaporated water continuously. Cyclones that form north of the equator spin counterclockwise whereas cyclones south of the equator spin clockwise due to the difference in Earth's rotation on its axis.

Storm surges from cyclones are generated due to an interaction between air and water. The atmosphere forces the water body and consequently oscillations are generated in the water body with periods ranging from a few minutes to a few days. A cyclone becomes deadly by causing inundation along the coastline if the maximum surge coincides with a high astronomical tide.

There are essentially two major forcing factors when a weather system moves over a water body:

a) Atmospheric pressure gradient normal to the sea surface. This is known as “inverse barometer effect” or “static amplification” or “the static part of the storm surge”. A decrease of one hectopascal (hPa) in the atmospheric pressure raises the sea level by one centimeter (cm). This static part has only about 5-15% contribution in the magnitude of a surge.

b) The dominant factor, known as “dynamic amplification”, is caused by the tangential wind stress (associated with the wind field of the weather system) acting over the sea surface which pushes the water towards the coast resulting to a pile-up of water at the coast.

The Saffir-Simpson Hurricane Wind Scale

The well-known Saffir-Simpson Hurricane Wind Scale [1] is designed to help determine wind hazards of an approaching hurricane easier for emergency officials. The scale is assigned five categories with Category 1 assigned to a minimal hurricane and Category 5 to a worst-case scenario. The Saffir-Simpson Scale classifying hurricane Category 1 to 5 is given in Table 1 [1]. Conditions for tropical depression and tropical storm are also provided in the table.

Table 1: Saffir-Simpson Hurricane Classification [1]

Storm type	**Category**	**Minimum pressure (hPa, mb)**	**1-minute maximum sustained wind speed**				**Surge (m)**	**Damage**
			knots	**mph**	**km/h**	**m/s**		
Tropical Depression	TD	-	< 34	<39	< 63	0-17	0	-
Tropical Storm	TS	-	34 – 63	39 – 73	63 – 118	18-32	0-0.9	-
Hurricane	1	> 980	64 – 82	74 – 95	119 – 153	33-42	1.0-1.7	Minimal
Hurricane	2	965 – 980	83 – 95	96 – 110	154 – 177	43-49	1.8-2.6	Moderate
Hurricane	3	945 – 965	96 – 113	111 – 130	178 – 210	50-58	2.7-3.8	Extensive
Hurricane	4	920 – 945	114 – 135	131 - 155	211 - 250	59-69	3.9-5.6	Extreme
Hurricane	5	< 920	> 135	> 155	> 250	>70	>5.7	Catastrophic

Damages from Typhoons

Typhoons are associated with high-pressure gradients and consequently generate strong winds, torrential rain and storm surges at landfall making these one of Earth’s most destructive natural phenomena. The destruction from a tropical cyclone depends on its intensity, size and location. Very strong winds may damage installations, dwellings, transportation and communication systems, trees etc. and cause fires resulting in considerable loss of life and damage to property and ecosystems. Cyclones also impose significant risks during construction and operation of seaports and other marine structures and facilities.

Typhoons have been responsible for the deaths of about 1.9 million people worldwide during the last two centuries. It is estimated that 10,000 people per year perish due to tropical cyclones [2]. Bangladesh is especially vulnerable to tropical cyclones with around 718,000 deaths from them in the past 50 years [3]. The deadliest tropical cyclone in Bangladesh was Cyclone Bhola (1970), which had a death toll of at least 300,000 [4] possibly as many as 500,000 [5, 6]. An estimated over 138,000 people were killed [7] with an equal number of injured [8] and about 13.4 million people were affected [8] by the 1991 Cyclone in Bangladesh.

During the 50 years since Cyclone Bhola, 1942 disasters were attributed to tropical cyclones worldwide which killed 779,324 people and caused US$ 1,407.6 billion in economic losses with an average of 43 deaths and US$ 78 million in damages every day [9].

Maximum damages from a cyclone occur if landfall takes place at high tide. There was a severe cyclone in the Bay of Bengal in October 1960 which claimed only over 5,000 lives [10] although the strength of this cyclone was like that of Cyclone Bhola (November 1970). The significant difference in fatalities is because the November 1970 cyclone crossed the coast at high tide while the October 1960 storm moved onshore at low tide [11].

A list of deadliest Pacific typhoons is provided in Table 2 [12]. The August 1931 China typhoon in 1931 killed 300,000 [13] as reported in [12]. Typhoon Nina in 1975 killed 229,000 [14] as reported in [12]. The costliest known Pacific typhoons (adjusted for inflation) are shown in Table 3 [15] as reported in [16]. Tables 4 and 5 show the deadliest [17] and costliest [18] hurricanes in the Atlantic Ocean. A list of the deadliest cyclones in the Northern Indian Ocean is provided in Table 6 [17].

Table 2: Deadliest Pacific typhoons [12]

Rank	Typhoon	Season	Fatalities
1	August 1931 China typhoon	1931	300,000
2	Nina	1975	229,000
3	July 1780 Typhoon	1780	100,000
4	July 1862 Typhoon	1862	80,000
5	Shantou	1922	60,000
6	China	1912	50,000
7	Hong Kong	1937	10,000
8	Joan	1964	7,000
9	Haiyan	2013	6,352
10	Vera	1959	>5,000

Table 3: Costliest known Pacific typhoons [15]

Rank	Typhoon	Season	Damage (2023 USD)
1	Doksuri	2023	$28.4 billion
2	Mireille	1991	$22.4 billion
3	Hagibis	2019	$20.6 billion
4	Jebi	2018	$17.0 billion
5	Yagi	2024	$16.5 billion
6	Songda	2004	$15.0 billion
7	Fitow	2013	$13.6 billion
8	Faxai	2019	$11.9 billion
9	Saomai	2000	$11.1 billion
10	Lekima	2019	$11.1 billion

Table 4: Deadliest Atlantic hurricanes [17]

Rank	Hurricane	Category	Season	Fatalities
1	Great Hurricane	?	1780	22,000–27,501
2	Mitch	5	1998	11,374+
3	Fifi	2	1974	8,210–10,000
4	Galveston	4	1900	8,000–12,000
5	Flora	4	1963	7,193
6	Pointe-à-Pitre	?	1776	6,000+
7	Okeechobee	5	1928	4,112+
8	Newfoundland	?	1775	4,000–4,163
9	Monterrey	3	1909	4,000
10	San Ciriaco	4	1899	3,855

Table 5: Costliest Atlantic hurricanes [18]

Rank	Hurricane	Category	Season	Damage
1	Katrina	5	2005	$125 billion
2	Harvey	4	2017	$125 billion
3	Ian	5	2022	$113 billion
4	Maria	5	2017	$91.6 billion
5	Irma	5	2017	$77.2 billion
6	Ida	4	2021	$75.3 billion
7	Sandy	3	2012	$68.7 billion
8	Ike	4	2008	$38 billion
9	Andrew	5	1992	$27.3 billion
10	Ivan	5	2004	$26.1 billion

Table 6: Deadliest cyclones in the Northern Indian Ocean [17]

Rank	Name/Year	Region	Fatalities
1	Bhola 1970	Bangladesh	>300,000
2	Unnamed 1582	Bangladesh	200,000
3	Unnamed 1876	Bangladesh	200,000
4	Unnamed 1897	Bangladesh	175,000

5	Bangladesh 1991	Bangladesh	138,866
6	Nargis 2008	Myanmar	138,373
7	Unnamed 1911	Bangladesh	120,000
8	Unnamed 1847	Bangladesh	75,000
9	Unnamed 1917	Bangladesh	70,000
10	Unnamed 1699	Bangladesh	50,000
11	Unnamed 1767	Bangladesh	50,000
12	Unnamed 1822	Bangladesh	50,000
13	Unnamed 1919	Bangladesh	40,000
14	Unnamed 1831	Bangladesh	22,000
15	Unnamed 1965	Bangladesh	19,270
16	Unnamed 1965	Bangladesh	12,000
17	Unnamed 1958	Bangladesh	12,000
18	Unnamed 1963	Bangladesh	11,520
19	Unnamed 1961	Bangladesh	11,468
20	Unnamed 1985	Bangladesh	11,069
21	Unnamed 1971	Bangladesh, India	11,000
22	Unnamed 1961	Bangladesh	10,466
23	Unnamed 1965	Pakistan	10,000
24	Unnamed 1977	India	10,000
25	Unnamed 1999	Bangladesh, India, Myanmar	9,899
26	Unnamed 1960	Bangladesh	8,149
27	Unnamed 1941	Bangladesh	7,000
28	Unnamed 1988	Bangladesh, India	6,240
29	Unnamed 1999	Pakistan	6,200
30	Unnamed 1960	Bangladesh	6,000

Benefits from Typhoons

Despite their devastating effects, tropical cyclones are essential features of the Earth's atmosphere as they bring rain to dry areas and transfer heat and energy from the equator to the cooler regions nearer the poles.

Impact of Climate Change on Typhoons

The observed and the projected impacts of climate change on tropical cyclones presented in this section were obtained from the Intergovernmental Panel on Climate Change (IPCC) [19].

<u>Past Observations [19]</u>

Globally the frequency of tropical cyclones has not increased and in fact the number may have fallen. However, it is likely that a higher proportion of tropical cyclones across the globe are reaching category three or above meaning these reach the highest wind speeds. The frequency and magnitude of rapid intensification has likely increased. This is where maximum wind speeds increase very quickly which can be especially dangerous. In some places, the average location where tropical cyclones reach their peak intensity has shifted poleward exposing new communities to these hazards. There also seems to have been a slowdown in the speed at which tropical cyclones move across the Earth's surface. This typically brings more rainfall for a given location. There has been an increase in the average and peak rainfall rates associated with tropical cyclones. There is high confidence that humans have contributed to increases in precipitation associated with tropical cyclones and medium confidence that humans have contributed to the higher probability of a tropical cyclone being more intense.

<u>Future Projections [19]</u>

Rising temperatures affect tropical cyclones in several ways such as a) warmer ocean waters mean cyclones can pick up more energy leading to higher wind speeds b) a warmer atmosphere can hold more moisture leading to more intense rainfall and c) sea-levels are rising due to melting glaciers and ice sheets; storm surges from tropical cyclones on the top of already elevated sea levels worsen coastal flooding. The number of tropical cyclones globally is unlikely to increase. However, as the world warms, it is very likely that these will have higher rates of rainfall and reach higher top wind speeds. This means a higher proportion would reach the most intense categories four and five. The more global temperatures rise, the more extreme these changes will be. The proportion of tropical cyclones reaching categories four and five may increase by around 10% if global temperature rises are limited to 1.5°C, increasing to 13% at 2°C and 20% at 4°C.

Major Typhoons in the Philippines

The Philippines is a typhoon-prone country with approximately 20 typhoons each year. Typhoons regularly form in the Philippine Sea and less regularly in the West Philippine Sea. June to September are the most active months and August being the month with the most activity. Each year at least ten typhoons are expected to hit the island nation with five expected to be destructive and powerful [20]. The Philippines is the most exposed country in the world to tropical storms [21].

Typhoons typically make an east-to-west route in the Philippines heading north or west due to the Coriolis force effect. As a result landfalls occur in the regions of the country that face the Pacific Ocean especially Eastern Visayas, Bicol Region, and northern Luzon whereas Mindanao is largely free of typhoons [21]. Typhoon activity in the Philippines reaches to a minimum in May before increasing steadily to June and spiking from July to September with August being the most active month for tropical cyclones. Activity reduces significantly in October [22]. Climate change is likely to worsen the situation with extreme weather events including typhoons posing various risks and threats to the Philippines [23].

The Philippines was hit by 565 natural disasters since 1990 that claimed the lives of more than 70,000. Millions are left homeless by each extreme weather event, with their livelihoods destroyed and clean water and food in short supply. Each year an average of 20 typhoons make landfall leaving affected communities repeatedly grappling with hunger, disease, and chronic poverty [24].

Figure 1 shows the tracks of tropical cyclones worldwide (1945–2006) [25]. The Philippines is under the red and yellow tracks (which indicates stronger intensity) northeast of Borneo in the figure. Tables 7, 8 and 9 respectively show the deadliest, costliest, and wettest typhoons in the Philippines [26].

The tables suggest that the deadliest typhoon was Typhoon Yolanda (Haiyan) in 2013 killing 6,300 [27] as reported in [26]. This typhoon was also the costliest event with an estimated damage of $2.2 billion [28] as reported in [26]. The wettest typhoon was the July 1911 typhoon with total precipitation of 2,210mm in Baguio [29] as reported in [26]. The tables suggest that the deadliest typhoons are not necessarily the costliest or the wettest. Information in this section was obtained from Wikipedia [26].

Table 7: Deadliest typhoons in the Philippines [26]

Rank	Typhoon	Season	Fatalities
1	Yolanda (Haiyan)	2013	6,300
2	Uring (Thelma)	1991	5,101–8,000
3	Pablo (Bopha)	2012	1,901
4	Angela	1867	1,800
5	Winnie	2004	1,593
6	October 1897	1897	1,500
7	Nitang (Ike)	1984	1,426
8	Reming (Durian)	2006	1,399
9	Frank (Fengshen)	2008	1,371
10	Washi (Sendong)	2011	1,257

Table 8: Costliest typhoons in the Philippines [26]

Rank	Typhoon	Season	Damage (USD)
1	Yolanda (Haiyan)	2013	2.2 billion
2	Odette (Rai)	2021	1.02 billion
3	Pablo (Bopha)	2012	1.06 billion
4	Glenda (Rammasun)	2014	771 million
5	Ompong (Mangkhut)	2018	627 million
6	Pepeng (Parma)	2009	581 million
7	Ulysses (Vamco)	2020	418 million
8	Rolly (Goni)	2020	369 million
9	Paeng (Nalgae)	2022	321 million
10	Pedring (Nesat)	2011	356 million

Table 9: Wettest typhoons in the Philippines [26]

Rank	Typhoon	Season	Precipitation	
			mm	Location
1	July 1911 cyclone	1911	2,210	Baguio
2	Pepeng (Parma)	2009	1,854	Baguio
3	Trining (Carla)	1967	1,216	Baguio
4	Iliang (Zeb)	1998	1,116	La Trinidad, Benguet
5	Feria (Utor)	2001	1,086	Baguio
6	Lando (Koppu)	2015	1,078	Baguio
7	Igme (Mindulle)	2004	1,013	-
8	Dante (Kujira)	2009	902	-

9	September 1929 typhoon	1929	880	Virac, Catanduanes
10	Openg (Dinah)	1977	870	Western Luzon

The recent Typhoon Gaemi (known in the Philippines as Super Typhoon Carina) was a powerful and destructive tropical cyclone that impacted East China after severely affecting Taiwan and the Philippines in late July 2024. Strong winds and heavy rainfalls during Typhoon Gaemi caused widespread flash flooding, landslide and damages to people and properties in the Philippines, Taiwan, China and Vietnam. Total deaths were 126 and total damages were $253 million in these countries [30].

The Present Study

Typhoon Haiyan (2013), known in the Philippines as Super Typhoon Yolanda, was the deadliest and costliest typhoon in the Philippines and, therefore, this paper has focused to this event.

Raw data (such as track, wind speed, pressure, and radius of maximum wind speed) were obtained from the International Best Track Archive for Climate Stewardship (IBTrACS) [31]. Two-dimensional wind and pressure fields along the entire track were then generated using the Cyclone Wind Generation Tool developed by DHI [32]. Two-dimensional wind and pressure fields at selected locations along the track are presented in this paper. Time-series wind speed and pressure over the entire passage of the typhoon are also provided at these selected locations.

The wind and pressure fields presented in this paper are useful for numerical modelling of waves and surge. Structural design considerations and cyclone risk reduction measures are also described in this paper. The methodology described in this paper for generating wind and pressure fields from Typhoon Haiyan could also be applied for other typhoons around the world.

TYPHOON HAIYAN (2013)

Formation of Typhoon Haiyan

Typhoon Haiyan (2-11 November 2013), known in the Philippines as Super Typhoon Yolanda, was one of the most powerful tropical cyclones ever recorded. Haiyan devastated portions of Southeast Asia, particularly the Philippines upon making landfall. It is one of the deadliest typhoons in the Philippines on record killing at least 6,300 people in that country alone. Haiyan is tied with Meranti in 2016 for being the second strongest landfalling tropical cyclone on record, only behind Goni of 2020. Haiyan was also the most intense tropical cyclone worldwide during 2013.

On 2 November, the Joint Typhoon Warning Center (JTWC) [33] began monitoring a broad low-pressure area about 425 kilometers (264 miles) east-southeast of Pohnpei, one of the states in the Federated States of Micronesia. As the system moved through a region favouring tropical cyclogenesis the Japan Meteorological Agency (JMA) [34] classified it as a tropical depression early on 3 November. JMA classified Haiyan as a typhoon on 5 November. JTWC estimated the storm to have attained Category 5-equivalent super typhoon status on the Saffir–Simpson hurricane wind scale (SSHWS) [1] around 12:00 UTC on 6 November. Around 12:00 UTC on 7 November, Haiyan attained ten-minute sustained winds of 230 km/h (140 mph) and a minimum central pressure of 895 mbar (hPa). Six hours later, the JTWC estimated Haiyan to have attained one-minute sustained winds of 315 km/h (196 mph) and gusts up to 380 km/h (240 mph). At 20:40 UTC on 7 November, Haiyan made landfall in Guiuan, Eastern Samar at peak intensity. The JTWC's unofficial estimate of one-minute sustained winds of 305 km/h (190 mph) would make Haiyan the most powerful storm ever recorded to strike land. This record was later broken by Typhoon Goni in 2020.

Typhoon Haiyan, with its core disrupted by land interaction with the Philippines, emerged over the South China Sea late on 8 November. Continuing across the South China Sea, Haiyan turned more northwesterly late on 9 November and through 10 November, as it moved around the southwestern edge of the subtropical ridge previously steering it westward. Rapid weakening ensued as Haiyan approached its final landfall in Vietnam, ultimately moving ashore in the country near Haiphong around 21:00 UTC, as a severe tropical storm. Once onshore, the storm quickly deteriorated and was last noted as it dissipated over Guangxi Zhuang Autonomous Region, China, on 11 November. The information in this section was obtained from Wikipedia [35].

Damages from Typhoon Haiyan

Strong winds and heavy rainfalls during Typhoon Haiyan caused widespread flash flooding, landslide and damages to people and properties in the Philippines, Vietnam, Mainland China, and Taiwan. Deaths and missing by country are provided in Table 10 [35].

Table 10: Deaths and missing from Typhoon Haiyan by country [35]

Country	Deaths	Missing
Philippines	6,300	1,061
Vietnam	14	4
Mainland China	30	6
Taiwan	8	0
Total	6,352	1,071

Track and Data of Typhoon Haiyan

The track (route) of Typhoon Haiyan was obtained from [31, 36] and is shown in Figure 2. The cyclone data was obtained from IBTrACS [31]. The IBTrACS archived cyclone data contains 3-hourly information including date and time, track (path) and the maximum sustained wind speeds (1-minute mean). Data on Typhoon Haiyan is provided in Table 11 [31]. Figures 3 and 4 show respectively the wind and central pressure intensity and radial wind information for Typhoon Haiyan obtained from IBTrACS [31].

Table 11: Track and data of Typhoon Haiyan (2013) [31]

Date and Time [UTC]	Latitude [°N]	Longitude [°E]	Max 1-minute wind speeds [knots]	Central Pressure [hPa]	Radius of maximum winds [nm]
03/11/2013 06:00	6.3	155.7	25	1004	45
03/11/2013 09:00	6.5	155.0	28	1002	45
03/11/2013 12:00	6.6	154.3	30	1000	45
03/11/2013 15:00	6.5	153.6	30	1000	45
03/11/2013 18:00	6.3	152.9	30	1000	45
03/11/2013 21:00	6.2	152.2	33	998	45
04/11/2013 00:00	6.1	151.5	35	996	45
04/11/2013 03:00	6.1	150.8	38	995	40
04/11/2013 06:00	6.1	150.1	40	993	35
04/11/2013 09:00	6.2	149.4	43	991	35
04/11/2013 12:00	6.3	148.7	45	989	35
04/11/2013 15:00	6.4	148.0	50	986	30
04/11/2013 18:00	6.4	147.2	55	982	25
04/11/2013 21:00	6.4	146.4	63	976	20
05/11/2013 00:00	6.4	145.7	70	970	15
05/11/2013 03:00	6.4	144.9	73	969	15
05/11/2013 06:00	6.5	144.2	75	967	15
05/11/2013 09:00	6.7	143.6	83	962	15
05/11/2013 12:00	6.9	142.9	90	956	15
05/11/2013 15:00	7.0	142.1	100	949	11
05/11/2013 18:00	7.1	141.3	110	941	7
05/11/2013 21:00	7.2	140.5	120	934	7
06/11/2013 00:00	7.3	139.7	130	926	7
06/11/2013 03:00	7.4	138.9	133	924	7
06/11/2013 06:00	7.6	138.0	135	922	7
06/11/2013 09:00	7.7	137.1	143	917	7
06/11/2013 12:00	7.9	136.1	150	911	7
06/11/2013 15:00	8.0	135.2	153	909	10
06/11/2013 18:00	8.2	134.3	155	907	12
06/11/2013 21:00	8.4	133.5	155	907	14
07/11/2013 00:00	8.7	132.7	155	907	15
07/11/2013 03:00	9.0	131.9	158	905	16
07/11/2013 06:00	9.4	131.0	160	903	17
07/11/2013 09:00	9.8	130.0	165	899	17
07/11/2013 12:00	10.2	129.0	170	895	17
07/11/2013 15:00	10.4	128.0	170	895	17
07/11/2013 18:00	10.6	126.9	170	895	17
07/11/2013 21:00	10.8	125.8	168	897	16
08/11/2013 00:00	11.0	124.7	165	899	15
08/11/2013 03:00	11.2	123.6	155	907	13
08/11/2013 06:00	11.4	122.5	145	914	10
08/11/2013 09:00	11.6	121.5	138	920	13
08/11/2013 12:00	11.8	120.4	130	926	15
08/11/2013 15:00	12.1	119.1	125	930	13
08/11/2013 18:00	12.4	117.9	120	933	10
08/11/2013 21:00	12.5	117.0	118	935	13
09/11/2013 00:00	12.6	116.2	115	937	15
09/11/2013 03:00	12.9	115.4	110	941	15

09/11/2013 06:00	13.4	114.6	105	944	15
09/11/2013 09:00	13.9	113.8	103	946	15
09/11/2013 12:00	14.5	113.1	100	948	15
09/11/2013 15:00	15.0	112.3	98	950	13
09/11/2013 18:00	15.5	111.5	95	952	10
09/11/2013 21:00	16.0	110.7	93	954	13
10/11/2013 00:00	16.5	110.1	90	956	15
10/11/2013 03:00	17.2	109.6	85	960	15
10/11/2013 06:00	17.9	109.2	80	963	15
10/11/2013 09:00	18.6	108.6	80	963	18
10/11/2013 12:00	19.3	108.0	80	963	20
10/11/2013 15:00	19.9	107.6	75	967	20
10/11/2013 18:00	20.5	107.4	70	970	20
10/11/2013 21:00	21.1	107.3	65	974	25
11/11/2013 00:00	21.8	107.3	60	978	30
11/11/2013 03:00	22.5	107.5	53	984	30
11/11/2013 06:00	23.2	107.9	45	989	30

WIND AND PRESSURE FIELDS GENERATION

The MIKE21 Cyclone Wind Generation Tool developed by DHI [32] was used to generate the cyclonic wind and pressure fields for the passage of Typhoon Haiyan. The tool allows users to compute wind and pressure data due to tropical cyclones (hurricanes or typhoons). Several cyclone parametric models are included in the tool such as Young and Sobey model (1981) [37], Holland – single vortex model (1981), Holland – double vortex model (1980) [38] and Rankine vortex model. The Young and Sobey model (1981) [37] was used in the study. The Young and Sobey model (1981) [37] as below requires six input parameters (i.e., time, track, radius of maximum wind speed, maximum wind speed, central pressure, and neutral pressure). The other models require some additional parameters (such as Holland parameter B and Rankine parameter X) that need to be calculated using empirical relationships. This adds further uncertainty to the generated wind and pressure fields. Therefore, the other models were not used for this study.

It should be noted that the 1-minute mean wind speeds in Table 9 were converted into 1-hour mean using the methodology described in the World Meteorological Organisation (WMO) [39] for use in the Cyclone Wind Generation Tool. Usually, 1-hour mean wind speeds are used for numerical modelling of cyclone waves and surge.

According to Young and Sobey (1981) [37], the rotational wind gradient speed V_g at a distance r from the centre of the cyclone is given by:

$$V_g(r) = V_{max} \cdot \left(\frac{r}{R_{mw}}\right)^7 . exp\left(7\left(1-\frac{r}{R_{mw}}\right)\right) \qquad \text{for } r < R_{mw}$$

$$V_g(r) = V_{max} . exp\left((0.0025R_{mw} + 0.05)\left(1-\frac{r}{R_{mw}}\right)\right) \qquad \text{for } r \geq R_{mw}$$

Where, R_{mw} is the radius to maximum wind speed and V_{max} is the maximum wind speed.

Following the Shore Protection Manual (1984) [40], the pressure p is given by:

$$p(r) = p_c + (p_n - p_c). exp\left(-\frac{R_{mw}}{r}\right)$$

Where, p_c is the pressure at the storm centre or central pressure and p_n is the ambient surroundings pressure field or neutral pressure.

Three types of wind corrections are available in the Cyclone Wind Generation Tool of DHI [32] to reflect the cyclonic wind structure. These wind corrections are described below from the Scientific Documentation of the Cyclone Wind Generation Tool of DHI [32].

a) Geostrophic Correction

The parametric models usually provide wind information at the geostrophic or gradient wind level above the influence of the planetary boundary layer. This gradient wind speed (V_g) may be reduced to the standard surface reference level (V_{10}) by considering the effects of the boundary layers as below:

$$V_{10}(r) = K_m . V_g(r)$$

Where, $V_g(r)$ is the rotational gradient wind speed (m/s) at a distance r from the centre of the cyclone, V_{10} is the near-surface wind speed (m/s), and K_m is the boundary layer wind speed correction coefficient.

Three options are available in the DHI tool [32], namely no correction, constant correction, and Harper et al. (2001) [41]. Harper et al. (2001) [41] empirical formulation was used in the present study where K_m is dependent on V_g through a set of equations as below:

$$K_m = \begin{cases} 0.81 & for\ V_g < 6\ m/s \\ 0.81 - 2.96\ 10^{-3}(V_g - 6) & for\ 6 \leq V_g < 19.5 \\ 0.77 - 4.31\ 10^{-3}(V_g - 19.5) & for\ 19.5 \leq V_g < 45 \\ 0.66 & for\ V_g > 45\ m/s \end{cases}$$

b) Forward Motion Asymmetry

Cyclone winds circulate clockwise in the Southern Hemisphere and anti-clockwise in the Northern Hemisphere. The wind field is asymmetric so that winds are typically stronger to the left of cyclone's track and lower to the right due to the contribution of the cyclone movement.

Two options are available in the DHI tool to consider the forward motion asymmetry at surface level, namely no correction and Harper et al. (2001) [41]. Harper et al. (2001) [41] empirical formulation (as below) was used in the present study where the user must specify the proportion of the correction factor, delta (δ_{fm}) and the angle of maximum winds, theta max (θ_{max}). The proportion of the added forward cyclone speed (V_{fm}) can be adjusted using the correction factor delta (δ_{fm}). Theta max (θ_{max}) is measured relative to the cyclone movement direction. In the DHI tool, the cyclone movement direction and the cyclone speed are computed based on the position of the centre of the storm given in the best track data table.

$$V_{10}(r,\theta) = K_m . V_g(r) + \delta_{fm}.V_{fm}.cos(\theta_{max} - \theta)$$

c) Inflow Angle

All the parametric wind models described earlier assume a circular wind flow pattern which does not represent the observed surface wind directions. Friction effects between water and air cause a deflection of the wind direction towards the centre of the cyclone. Two options are available in the DHI tool, namely no correction and Sobey et al. (1977) [42]. Sobey et al. (1977) [42] empirical formulation (as below) was used in the present study where the deflection is characterised by the inflow angle (β) in the order of 25° but decreases towards the storm centre.

$$\beta = \begin{cases} 10\ \frac{r}{R_{mw}} & \text{for}\ \ 0 \leq r < R_{mw} \\ 10 + 75\left(\frac{r}{R_{mw}} - 1\right) & \text{for}\ \ R_{mw} \leq r < 1.2\ R_{mw} \\ 25 & \text{for}\ \ r \geq 1.2\ R_{mw} \end{cases}$$

RESULTS AND DISCUSSIONS

Two-dimensional wind and pressure fields were generated along the entire path of Typhoon Haiyan. Then two-dimensional wind and pressure fields at key selected locations were extracted. The selected locations are shown in Figure 5. Coordinates, hourly timesteps and date and time of these locations are provided in Table 12.

Table 12: Wind and pressure fields extraction locations, timesteps and date and time

Locations	Coordinates		Hourly timesteps	Date and time
	Latitude (°N)	Longitude (°E)		
P1	9.4	131.0	96	07/11/2013 06:00
P2	10.2	129.0	102	07/11/2013 12:00
P3	10.6	126.9	108	07/11/2013 18:00
P4	11.0	124.7	114	08/11/2013 00:00
P5	11.4	122.5	120	08/11/2013 06:00
P6	11.8	120.4	126	08/11/2013 12:00
P7	12.4	117.9	132	08/11/2013 18:00

The top plot in Figures 6 to 12 show the two-dimensional wind fields when the typhoon reached to locations P1 to P7 respectively. The time-series of wind speeds at these locations during the entire passage of the typhoon are presented at the bottom of these figures. Figure 13 compares the time-series of wind speeds at the selected locations during the entire passage of the typhoon.

The top plot in Figures 14 to 20 show the two-dimensional pressure fields when the typhoon reached to locations P1 to P7 respectively. The time-series of pressure at these locations during the entire passage of the typhoon are presented at the bottom of these figures. Figure 21 compares the time-series of pressure at the selected locations during the entire passage of the typhoon.

The highest wind speeds and the lowest pressures at the selected locations during the entire passage of Typhoon Haiyan are summarised in Table 13 from the time-series plots presented earlier and are also shown in Figure 22. The highest wind speed and the lowest pressure are found in P2 where the typhoon reached to its peak intensity. It should be noted that 1 Hectopascal (hPa) = 100 Pascals (Pa).

Table 13: The highest wind speeds and the lowest pressures at the selected locations

Locations	Highest wind speed (m/s)	Lowest pressure (hPa)
P1	47.8	903
P2	50.4	895
P3	49.6	895
P4	46.6	899
P5	40.4	914
P6	36.8	926
P7	34.5	933

RECOMMENDED DESIGN CONSIDERATIONS

The potential impact of a cyclone event on the design of coastal and marine facilities may be summarised as follows:

1) Shoaling results in an increase in water levels and stronger currents inshore. Measures will be required to protect structures from scouring of the foreshore and seabed and limit damage to the crest if heavy overtopping occurs;
2) The foreshore will be subjected to flooding as the cyclone waves and surge approach; and
3) Facilities located on the landward slope are at risk from cyclone wave run-up and surge.

TYPHOON RISK REDUCTION MEASURES

Risks Reduction from Typhoons

Damage due to a cyclone depends on the strength and proximity of the cyclone as well as local bathymetry and topography and the location of people, structures, and facilities. Damage due to a cyclone also depends on the landfall timing with a landfall during a high tide increases risks and damages.

It is almost impossible to fully protect people and settlements from major cyclonic events. However, various soft and hard measures (independently or in combination) could be adopted to reduce fatalities and damage to key infrastructure.

Some potential measures to reduce the risk of damage and deaths from major cyclonic events are highlighted below:

1) Detection, early warning systems and real-time observation systems are of great importance;
2) Appropriate awareness and understanding among the general public;
3) Mitigation plans and evacuation and rescue preparedness by responsible authorities;
4) Cyclone risk assessment, flood risk and inundation hazard maps;
5) Cyclone shelters;
6) Developing artificial forest such as mangroves and casuarinas of appropriate width behind the shoreline to reduce cyclone wave energy;

7) Maintaining natural sand dunes;
8) Regulations for development in the coastal zone;
9) Saline embankments to prevent salt-water entering into fertile lands;
10) Raising ground levels of important structures and facilities such as warehouses, terminals and quays; and
11) Constructing cyclone defence structures such seawalls, dykes, gates, nearshore breakwaters, and offshore barriers. However, these structures are substantial and very expensive.

For major coastal infrastructure, the adoption of appropriate design parameters, a proper assessment of structural loads, forces, and stability in combination with a detailed understanding of cyclone processes will reduce the level of damage resulting from these events. Furthermore, physical modelling of major coastal and marine structures and mooring systems to investigate their stability under severe conditions will be helpful to reduce damage due to cyclones.

Risks Reduction from Mudslides and Landslides

High tides and heavy and prolonged rains during a cyclone may cause floods and submergence of low-lying areas which may lead to mudslides and landslides in mountainous areas causing loss of life and property. Landslides and mudslides are downhill earth movements that move slowly and cause gradual damage. They can also move rapidly destroying property and taking lives suddenly and unexpectedly. They typically carry heavy debris such as trees and boulders which cause severe damage together with injury or death. Faster movement of mudslides makes them deadly.

It is not possible to prevent a mudslide or a landslide. However, preparatory steps can be taken to lessen the impact of a mudslide. Some guidelines are briefly mentioned below:

1) Carrying out risk assessment;
2) Creating public awareness and practicing an evacuation plan;
3) Staying up to date on storm/rainfall/cyclone warnings during times of increased risk;
4) Watching for any visible signs such as cracks on land, debris flows or trees tilting or boulders knocking;
5) Staying alert and awake;
6) Moving out of the path of the landslide or debris flow; and
7) Some erosion control measures might be helpful (such as installing barrier walls, improving drainage system and planting trees with deep and extensive root systems).

SUMMARY AND FINDINGS

Typhoon Haiyan (2013), known in the Philippines as Super Typhoon Yolanda, was the deadliest and costliest typhoon in the Philippines and, therefore, this paper has focused to this event.

Raw data (such as track, wind speed, pressure, and radius of maximum wind speed) were obtained from IBTrACS [31]. Two-dimensional wind and pressure fields along the entire track were then generated using the Cyclone Wind Generation Tool developed by DHI [32].

Two-dimensional wind and pressure fields at selected locations along the track are presented in this paper. Time-series wind speed and pressure during the entire passage of the typhoon are also provided at these selected locations.

The highest wind speeds and the lowest pressures at the selected locations are summarised both in tabular and graphical formats from the time-series plots at these locations. The highest wind speed and the lowest pressure were found at a location (P2) where the typhoon reached to its peak intensity.

The two-dimensional wind and pressure fields are useful for numerical modelling of waves and surge. Structural design considerations and cyclone risk reduction measures are also described in this paper. The methodology described in this paper for generating wind and pressure fields from Typhoon Haiyan could also be applied for other typhoons around the world.

ACKNOWLEDGEMENTS

The author would like to thank Royal HaskoningDHV (an independent, international engineering and project management consultancy company, www.royalhaskoningdhv.com) for giving permission to publish this paper. The author would like to thank his colleague Debra Griffin for carrying out the proof reading of this manuscript. The author would also like to thank the external reviewers who provided valuable comments to improve the paper.

REFERENCES

[1]. Simpson, R. H. (1974). The hurricane disaster--potential scale. Weatherwise, 27, 169. https://www.aoml.noaa.gov/general/WWW000/text/sfsimp.html.https://www.aoml.noaa.gov/hrd/Landsea/deadly/Table1.htm.

[2]. Adler, R. F. (2005). Estimating the benefit of TRMM tropical cyclone data in saving lives, June 20, 2005.

[3]. Ubydul Haque, Masahiro Hashizume, Korine N Kolivras, Hans J Overgaard, Bivash Das, and Taro Yamamotoa (2012). Reduced death rates from cyclones in Bangladesh: what more needs to be done?

Bulletin of the World Health Organization, 2012 Feb 1; 90(2): 150-156, PMCID: PMC3302549, published online 2011 Oct 24. doi: 10.2471/BLT.11.088302.

[4]. Arizona State University (2020). World: Highest Mortality, Tropical Cyclone. World Meteorological Organization's World Weather & Climate Extremes Archive. Arizona State University, November 12, 2020.

[5]. Business Insider India (2017). The 16 deadliest storms of the last century, Business Insider India, September 13, 2017.

[6]. Julian, F. (2019). Remembering the great Bhola cyclone, Dhaka Tribune, November 9, 2019.

[7]. Rudolph, D. K. and Guard, C. P. (1992). 1991 Annual Tropical Cyclone Report. U.S. Naval Oceanography Command Center, Joint Typhoon Warning Center, https://web.archive.org/web/20200813232009/https://www.usno.navy.mil/NOOC/nmfc-ph/RSS/jtwc/atcr/1991atcr.pdf.

[8]. United States Agency for International Development. The Bangladesh Cyclone of 1991 (PDF) (Report), United States Agency for International Development, https://pdf.usaid.gov/pdf_docs/Pnadg744.pdf.

[9]. WMO (2020). World’s deadliest tropical cyclone was50 years ago. World Meteorological Organization (WMO), Tags: Tropical cyclones, Disaster risk reduction, published 12 November 2020, member Bangladesh, https://wmo.int/media/news/worlds-deadliest-tropical-cyclone-was-50-years-ago.

[10]. Dunn, G., E. (1962). The tropical cyclone problem in East Pakistan. Mon. Wea. Rev., 91, 83-86.

[11]. Frank, Neil and Husain, S. A. (1971). The deadliest tropical cyclone in history? Bulletin of the American Meteorological Society. American Meteorological Society, volume 52, number 6, page 438-444, June 1971. Bibcode:1971BAMS...52..438F. doi:10.1175/1520-0477(1971)052<0438:TDTCIH>2.0.CO;2.

[12]. Wikipedia (2024a). Template:Deadliest typhoons. https://en.wikipedia.org/wiki/Template:Deadliest_typhoons.

[13]. Courtney, Chris (2018). The Nature of Disaster in China: The 1931 Yangzi River Flood. Cambridge University Press. ISBN 9781108284936, February 15, 2018.

[14]. NOAA (2009). The Worst Natural Disasters by Death Toll (PDF). National Oceanic and Atmospheric Administration, 2009. Retrieved January 2, 2012.

[15]. EM-DAT (2024). The International Disaster Database, https://www.emdat.be.

[16]. Wikipedia (2024). Typhoon Yagi. https://en.wikipedia.org/wiki/Typhoon_Yagi.

[17]. Wikipedia (2024b). List of the deadliest tropical cyclones. https://en.wikipedia.org/wiki/List_of_the_deadliest_tropical_cyclones.

[18]. Wikipedia (2024c). List of costliest Atlantic hurricanes. https://en.wikipedia.org/wiki/List_of_costliest_Atlantic_hurricanes.

[19]. Seneviratne, S.I., X. Zhang, M. Adnan, W. Badi, C. Dereczynski, A. Di Luca, S. Ghosh, I. Iskandar, J. Kossin, S. Lewis, F. Otto, I. Pinto, M. Satoh, S.M. Vicente-Serrano, M. Wehner, and B. Zhou, 2021: Weather and Climate Extreme Events in a Changing Climate. In Climate Change 2021: The Physical Science Basis. Contribution of Working Group I to the Sixth Assessment Report of the Intergovernmental Panel on Climate Change [Masson-Delmotte, V., P. Zhai, A. Pirani, S.L. Connors, C. Péan, S. Berger, N. Caud, Y. Chen, L. Goldfarb, M.I. Gomis, M. Huang, K. Leitzell, E. Lonnoy, J.B.R. Matthews, T.K. Maycock, T. Waterfield, O. Yelekçi, R. Yu, and B. Zhou (eds.)]. Cambridge University Press, Cambridge, United Kingdom and New York, NY, USA, pp. 1513–1766, doi:10.1017/9781009157896.013.

[20]. de la Cruz, Gwen (2016). IN NUMBERS: Typhoons in the Philippines and the 2016 polls (19 March 2016). Rappler. Retrieved April 12, 2017.

[21]. Brown, Sophie (2013). The Philippines Is the Most Storm-Exposed Country on Earth (11 November 2013). Time. Retrieved April 12, 2017.

[22]. García-Herrera, Ricardo; Ribera, Pedro; Hernández, Emiliano; Gimeno, Luis (2003). Typhoons in the Philippine Islands, 1566–1900 (PDF) (26 September 2003). David V. Padua. p. 40. Retrieved April 13, 2010.

[23]. Overland, Indra et al. (2017). Impact of Climate Change on ASEAN International Affairs: Risk and Opportunity Multiplier, Norwegian Institute of International Affairs (NUPI) and Myanmar Institute of International and Strategic Studies (MISIS).

[24]. Relief International Inc (2024). Relief International Inc, 1101 14th St., NW, Suite 710, Washington, D.C. 20005, United Sates. https://www.ri.org/countries/philippines?gad_source=1&gclid=EAIaIQobChMIloy4stDnhwMVhJRQBh28NibjEAAYAyAAEgJxJ_D_BwE.

[25]. Citynoise at English Wikipedia (2008). Tropical Cyclones, 1945–2006. Data from the Joint Typhoon Warning Center and the U.S. National Oceanographic and Atmospheric Administration. Colors based on Template talk:Storm colour. By Citynoise at English Wikipedia, CC BY-SA 3.0, March 2008. https://commons.wikimedia.org/w/index.php?curid=18049077.

[26]. Wikipedia (2024d). Typhoons in the Philippines. https://en.wikipedia.org/wiki/Typhoons_in_the_Philippines.
[27]. Del Rosario, Eduardo D [2011]. Final Report on Typhoon "Yolanda" (Haiyan) (PDF) (Report). Philippine National Disaster Risk Reduction and Management Council. pp. 77–148, 9 August 2011. Archived (PDF) from the original on November 5, 2020. Retrieved March 27, 2022.
[28]. del Rosario, Eduardo D. [2014]. FINAL REPORT Effects of Typhoon YOLANDA (HAIYAN) (PDF) (Report). NDRRMC, April 2014. Retrieved March 14, 2015.
[29]. Paulhaus, J. L. H. [1973]. World Meteorological Organization Operational Hydrology Report No. 1: Manual For Estimation of Probable Maximum Precipitation. World Meteorological Organization, 1973, p. 178.
[30]. Wikipedia (2024e). Typhoon Gaemi. https://en.wikipedia.org/wiki/Typhoon_Gaemi.
[31]. IBTrACS (2013). 2013 Super Typhoon HAIYAN (2013306N07162). International Best Track Archive for Climate Stewardship (IBTrACS). https://ncics.org/ibtracs/index.php?name=v04r01-2013306N07162.
[32]. DHI (2024). MIKE21 Cyclone Wind Generation Tool, Scientific Documentation, DK-2970, Hørsholm, Denmark, 2024.
[33]. JTWC (2024). Joint Typhoon Warning Center, A Joint United States Navy – United States Air Force command in Pearl Harbor, Hawaii. https://www.metoc.navy.mil/jtwc/jtwc.html.
[34]. JMA (2024). The Japan Meteorological Agency, Ministry of Land, Infrastructure, Transport and Tourism. https://www.jma.go.jp/jma/indexe.html.
[35]. Wikipedia (2024f). Typhoon Haiyan. https://en.wikipedia.org/wiki/Typhoon_Haiyan.
[36]. Deng, Jasper (2023). Track map of Typhoon Haiyan of the 2013 Pacific typhoon season. Map plotting the storm's track and intensity, according to the Saffir–Simpson scale showMap key. Created by Jasper Deng using Wikipedia:WikiProject Tropical cyclones/Tracks. The background image is from NASA. Tracking data is from NOAA (bwp312023.dat). Created: 2 November 2013, Uploaded: 14 September 2023. https://en.wikipedia.org/wiki/Typhoon_Haiyan#/media/File:Haiyan_2013_path.png.
[37]. Young, I.R. and Sobey, R.J. (1981). The numerical prediction of tropical cyclone wind-waves. James Cook University of North Queensland, Townville, Dept. of Civil & Systems Eng., Research Bulletin No. CS14.
[38]. Holland, G. (1980). An analytic model of the wind and pressure profiles in hurricanes. Monthly weather review, volume 108, pp. 1212-1218.
[39]. WMO (2008). Guidelines for converting between various wind averaging periods in tropical cyclone conditions, Appendix II, World Meteorological Organisation (WMO), October 2008.
[40]. Shore Protection Manual (1984). Department of the Army, US Army Corps of Engineers, Washington, DC 20314.
[41]. Harper, B.A., Hardy, T.A., Mason, L.B., Bode, L., Young, I.R., Nielsen, P. (2001). Queensland climate change and community vulnerability to tropical cyclones. Ocean Hazards Assessment – Stage 1, Report, Department of Natural Resources and Mines, Queensland, Brisbane, Australia, 368 p.
[42]. Sobey, R.J., Harper, B.A. and Stark, K.P. (1977). Numerical simulation of tropical cyclone storm surge. Research Bulletin CS-14, Dept Civil and Systems Engineering, James Cook University.

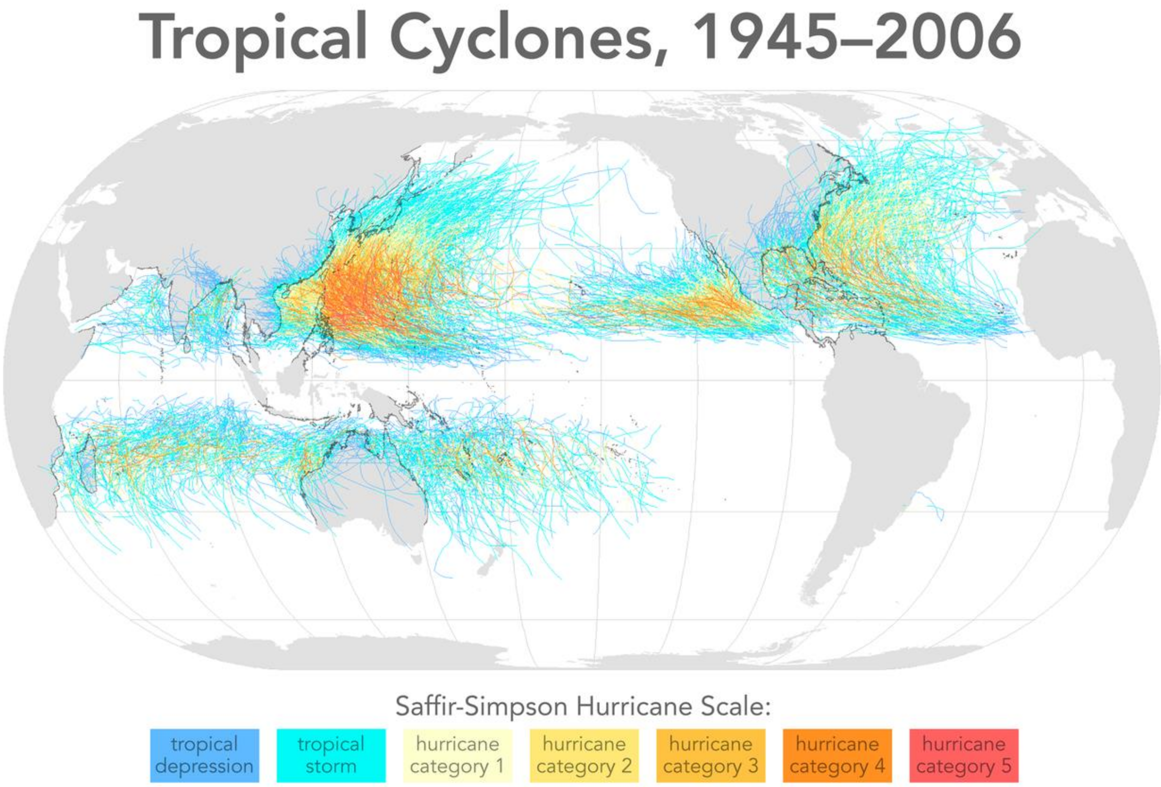

Figure 1: Tracks of tropical cyclones worldwide (1945–2006) [25]

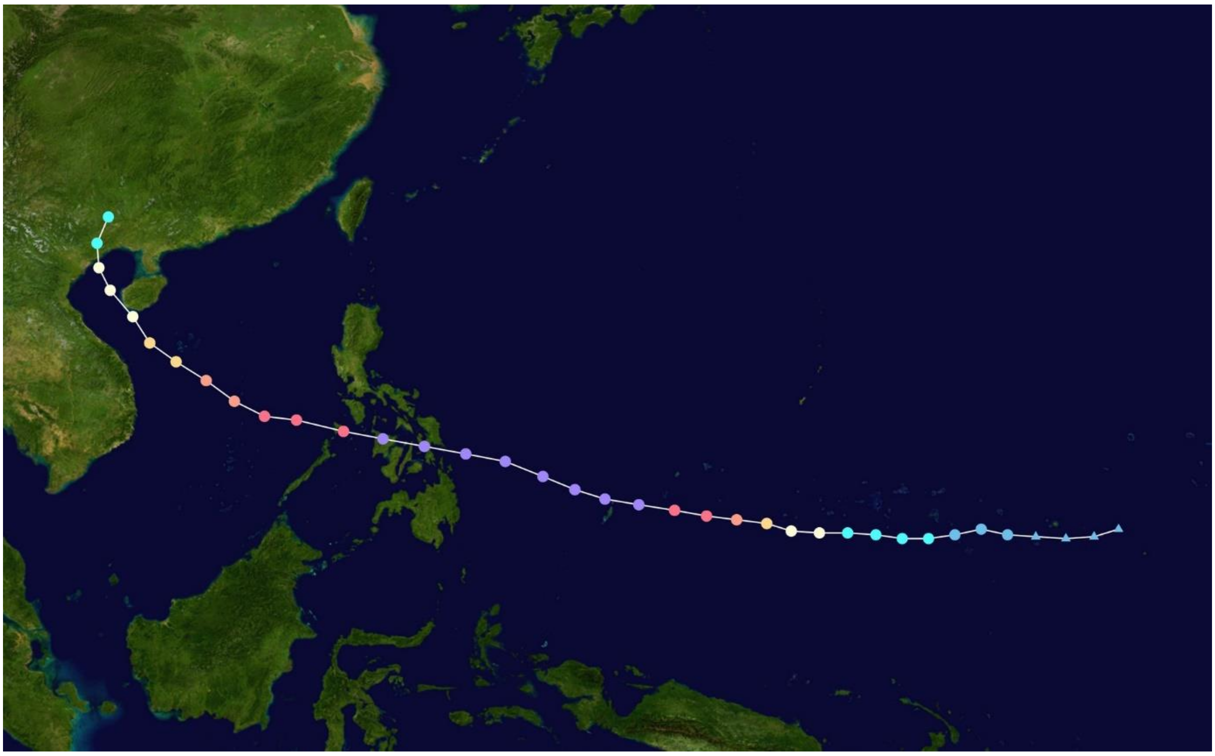

Figure 2a: Track of Typhoon Haiyan [36]

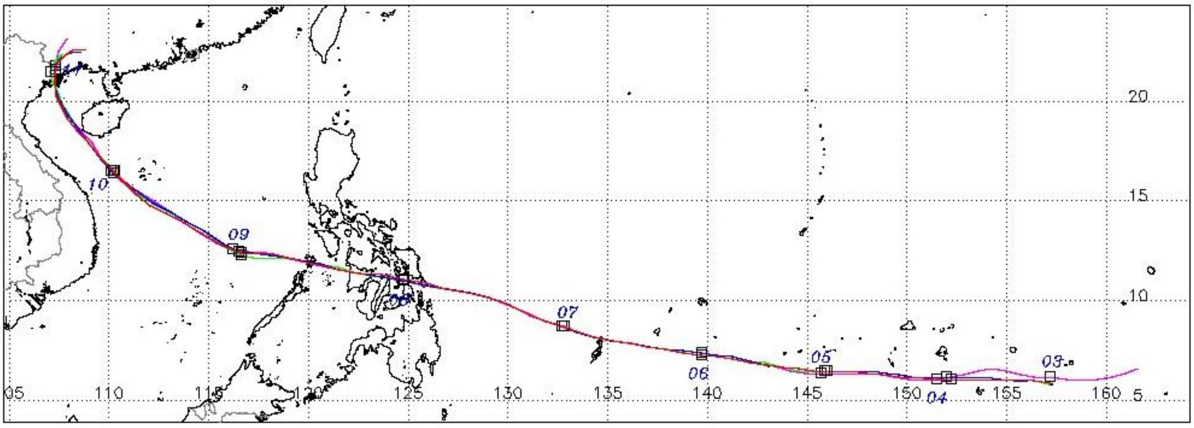

Figure 2b: Track of Typhoon Haiyan [31]

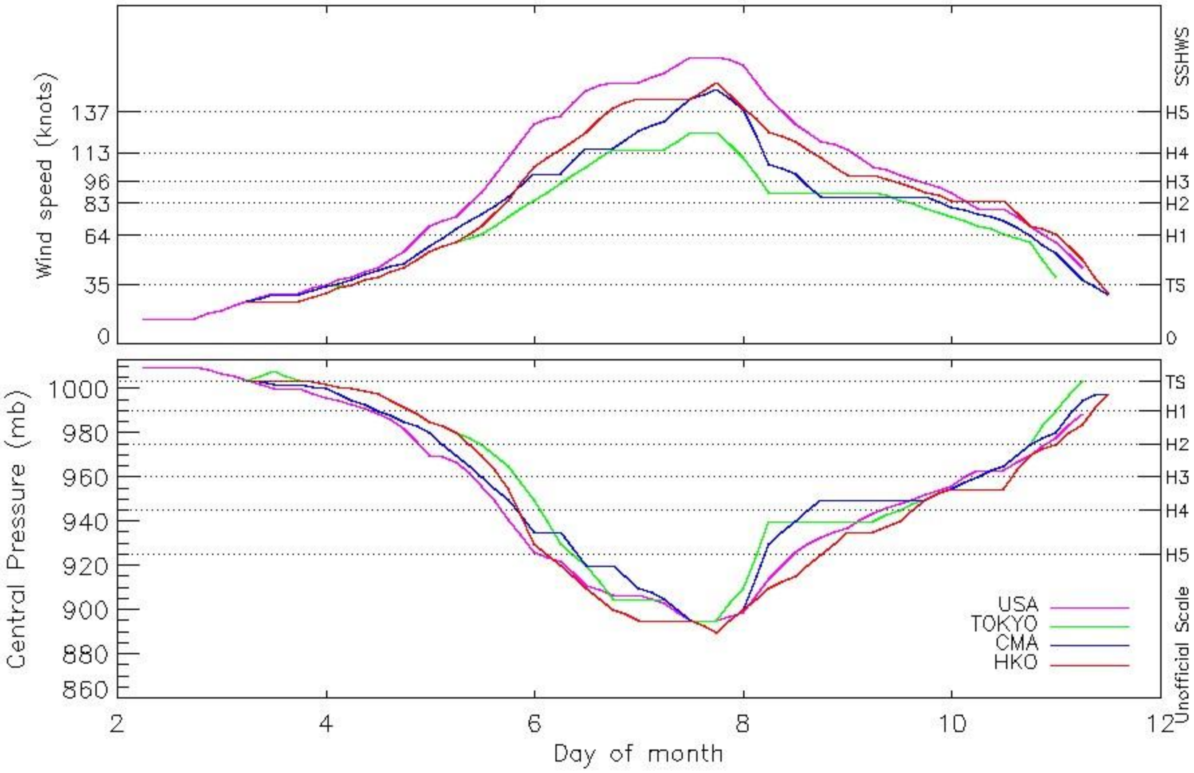

Figure 3: Wind and central pressure intensity plot of Typhoon Haiyan [31]

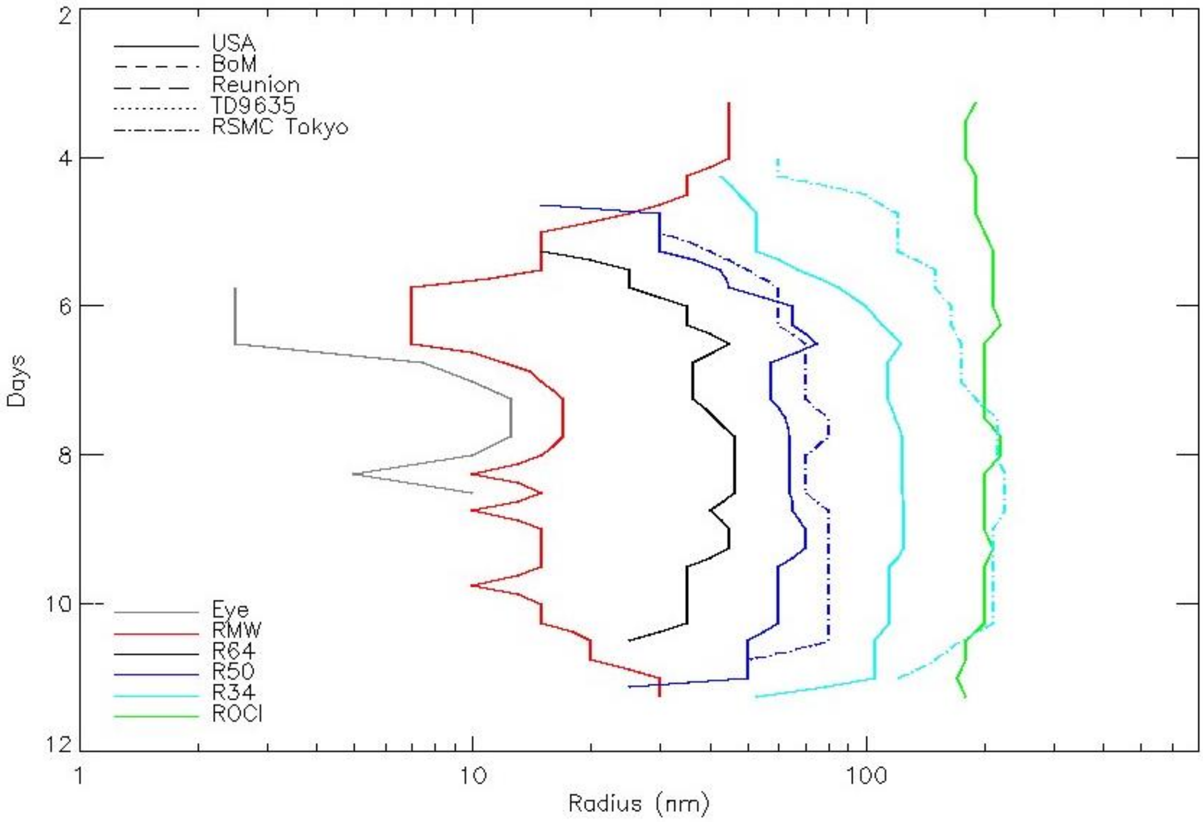

Figure 4: Radial wind information of Typhoon Haiyan [31]

Figure 5: Wind and pressure fields extraction locations

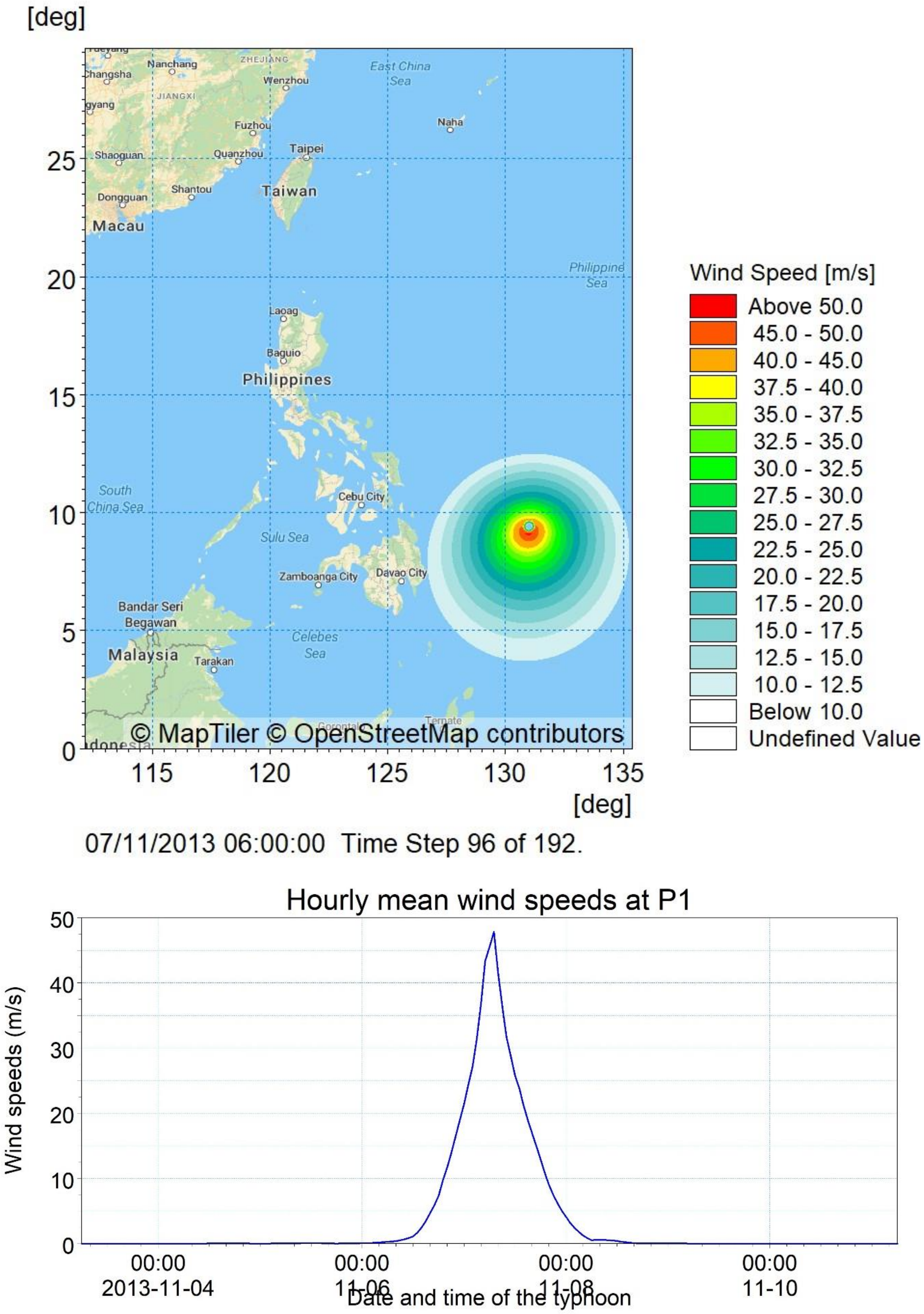

Figure 6: Wind field of Typhoon Haiyan at P1 (top – 2D wind field; bottom – time-series of wind speeds)

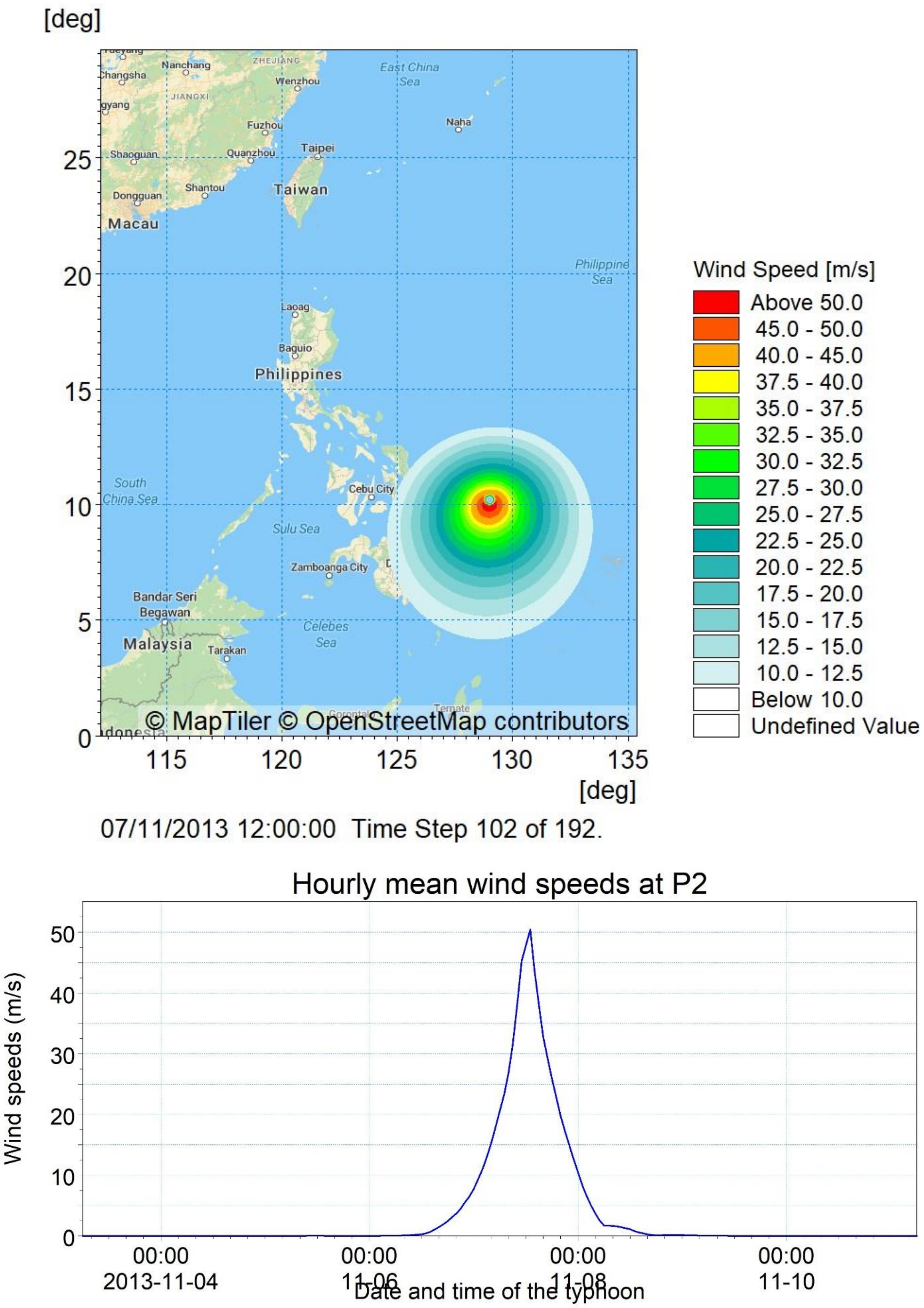

Figure 7: Wind field of Typhoon Haiyan at P2 (top – 2D wind field; bottom – time-series of wind speeds)

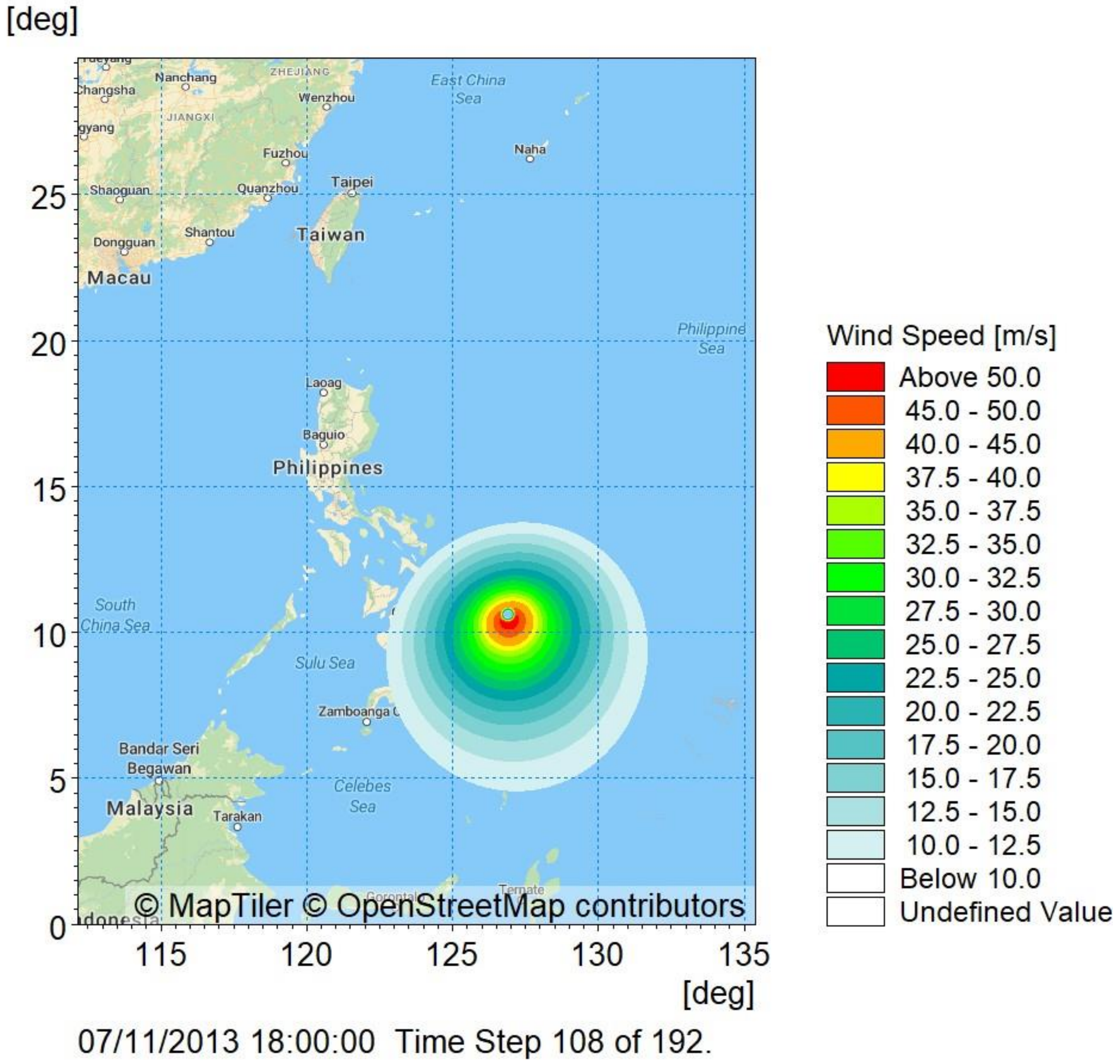

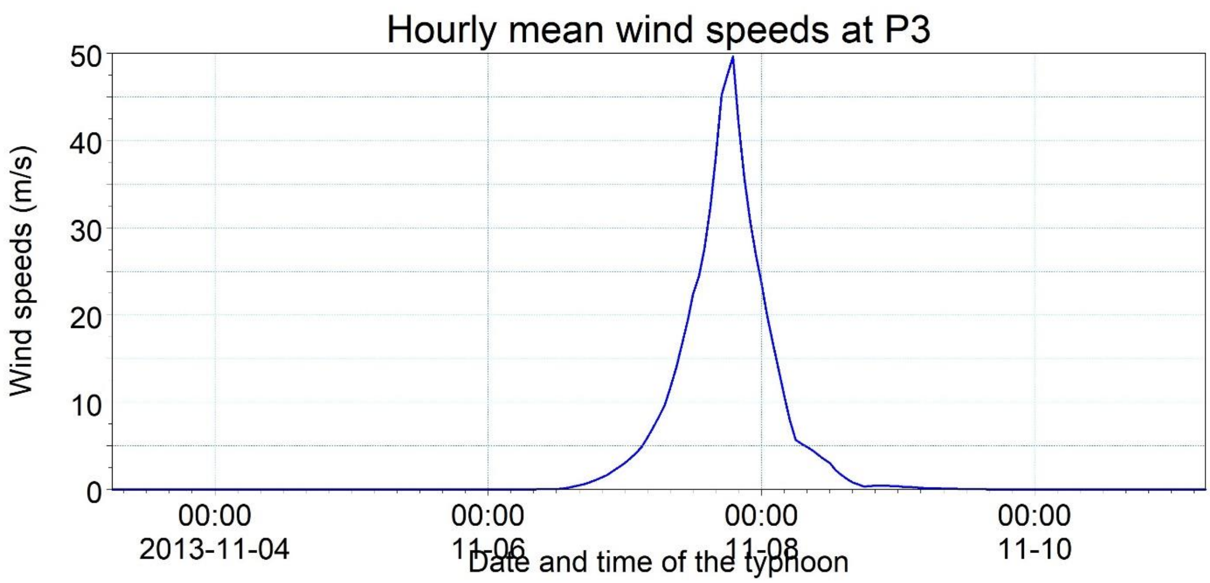

Figure 8: Wind field of Typhoon Haiyan at P3 (top – 2D wind field; bottom – time-series of wind speeds)

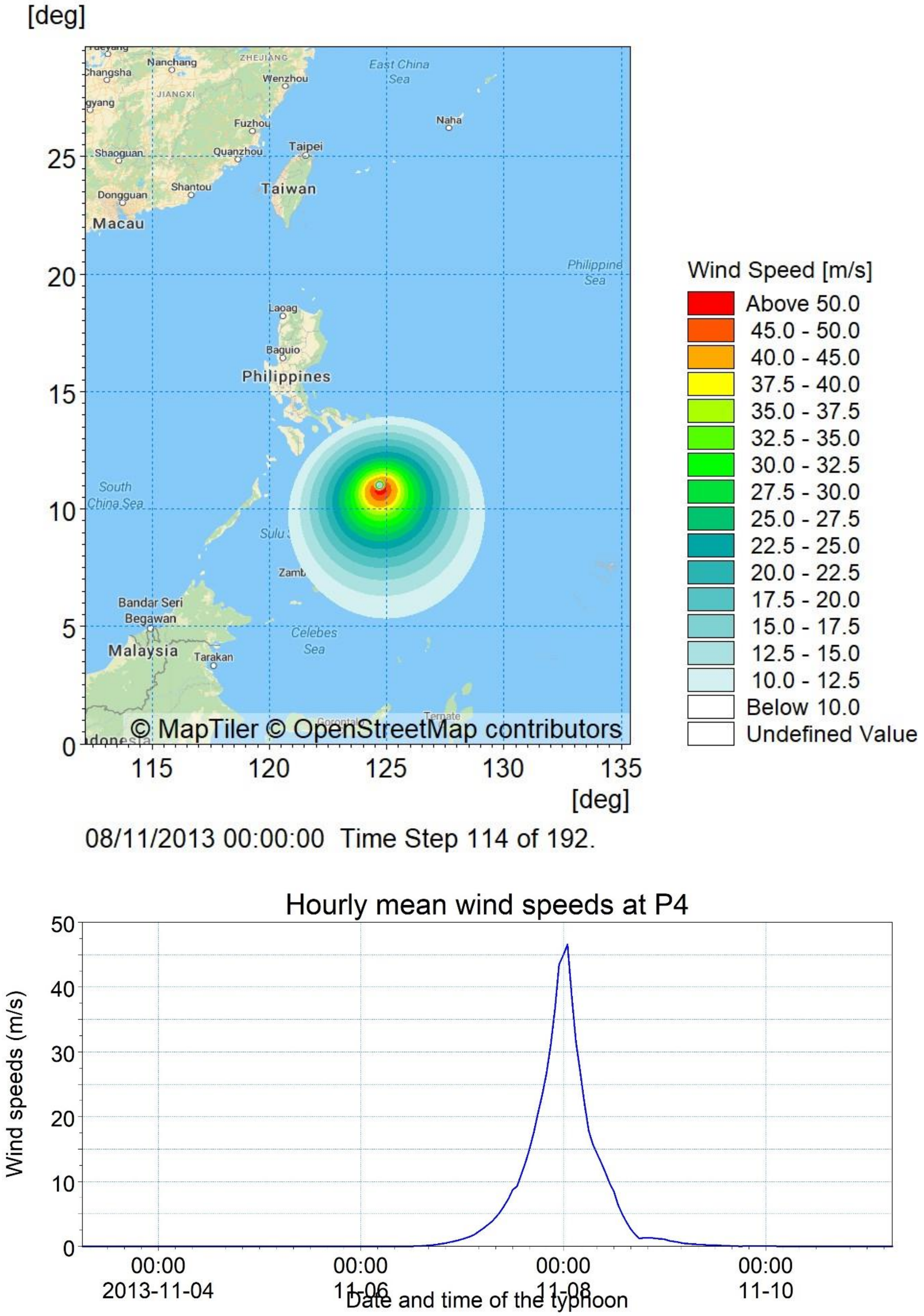

Figure 9: Wind field of Typhoon Haiyan at P4 (top – 2D wind field; bottom – time-series of wind speeds)

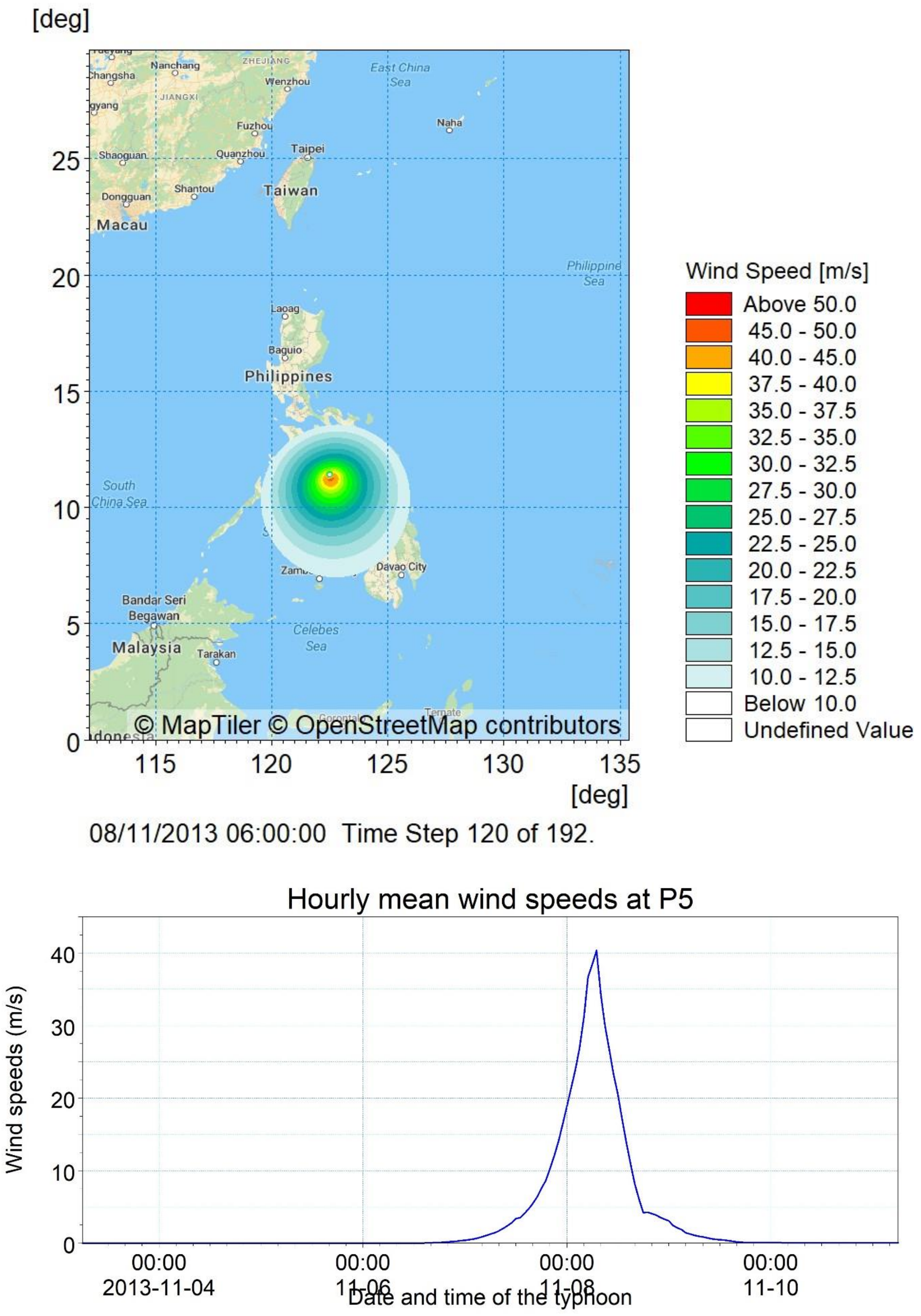

Figure 10: Wind field of Typhoon Haiyan at P5 (top – 2D wind field; bottom – time-series of wind speeds)

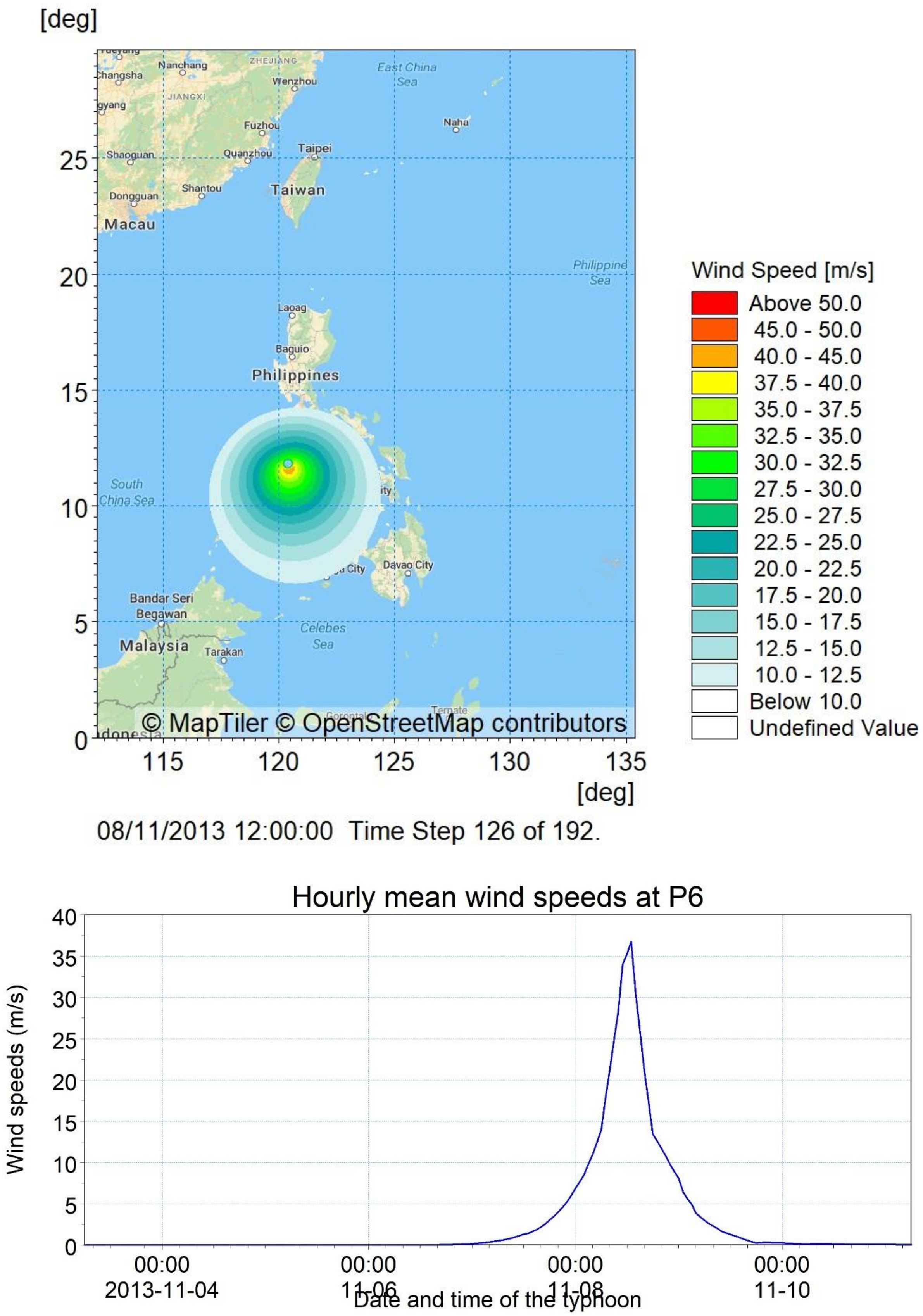

Figure 11: Wind field of Typhoon Haiyan at P6 (top – 2D wind field; bottom – time-series of wind speeds)

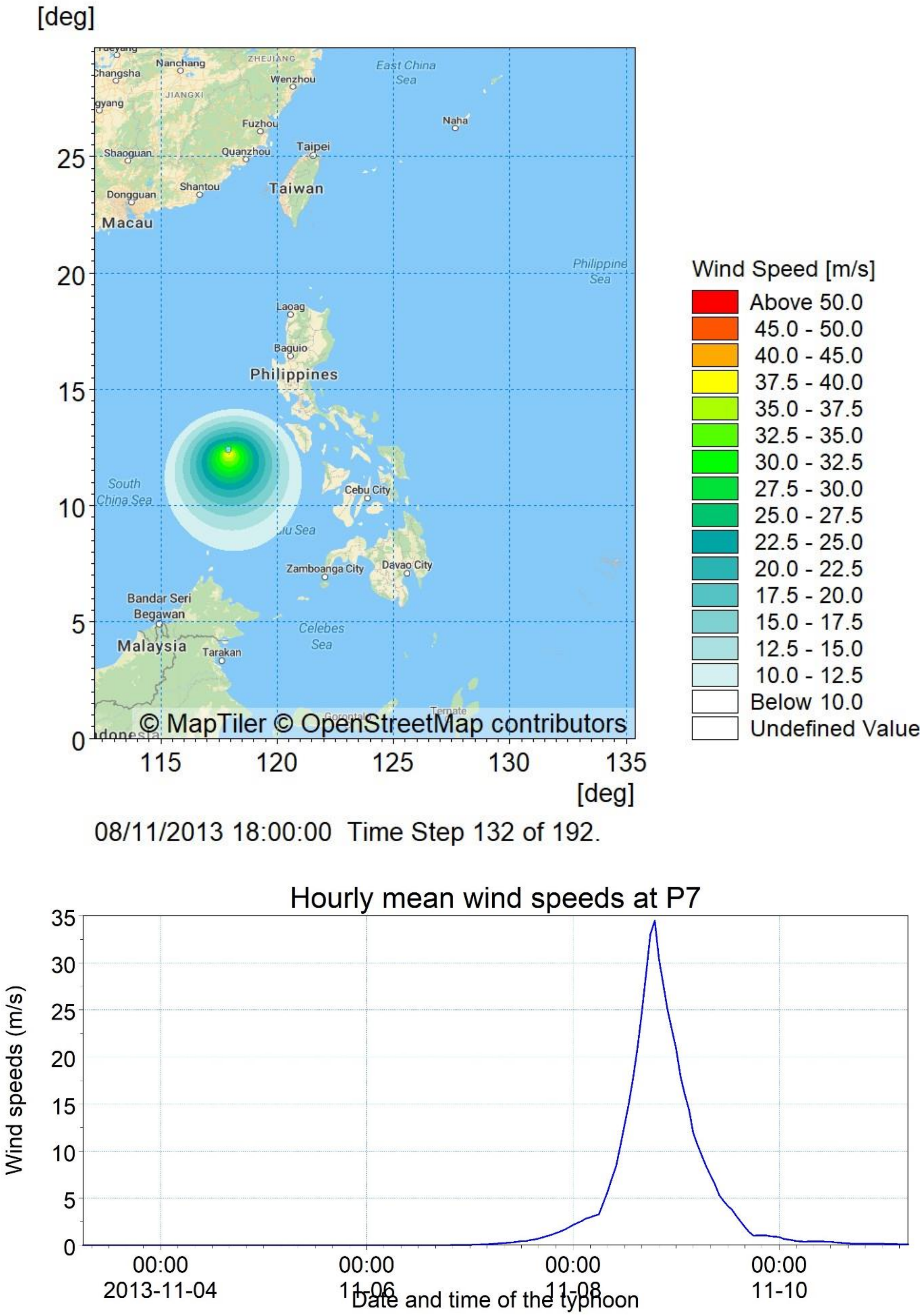

Figure 12: Wind field of Typhoon Haiyan at P7 (top – 2D wind field; bottom – time-series of wind speeds)

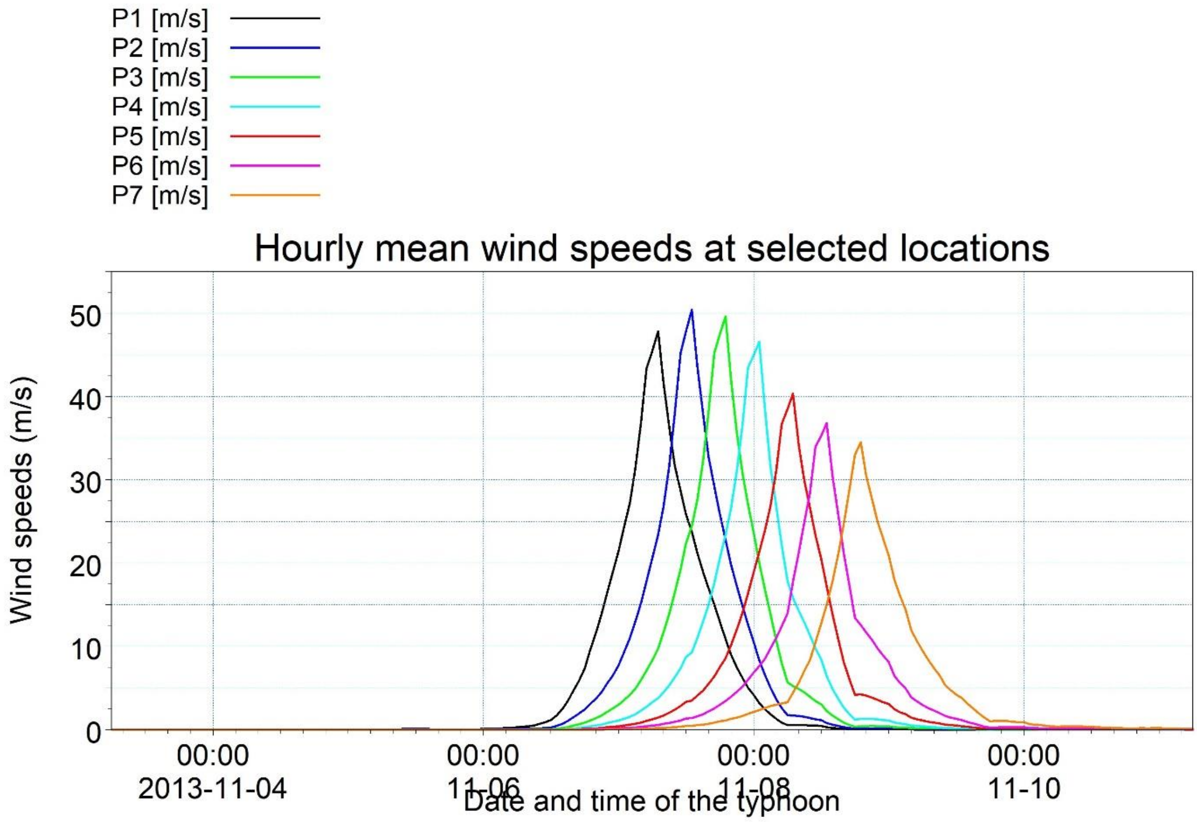

Figure 13: Time-series of hourly-mean wind speeds at the selected locations during the entire passage of Typhoon Haiyan

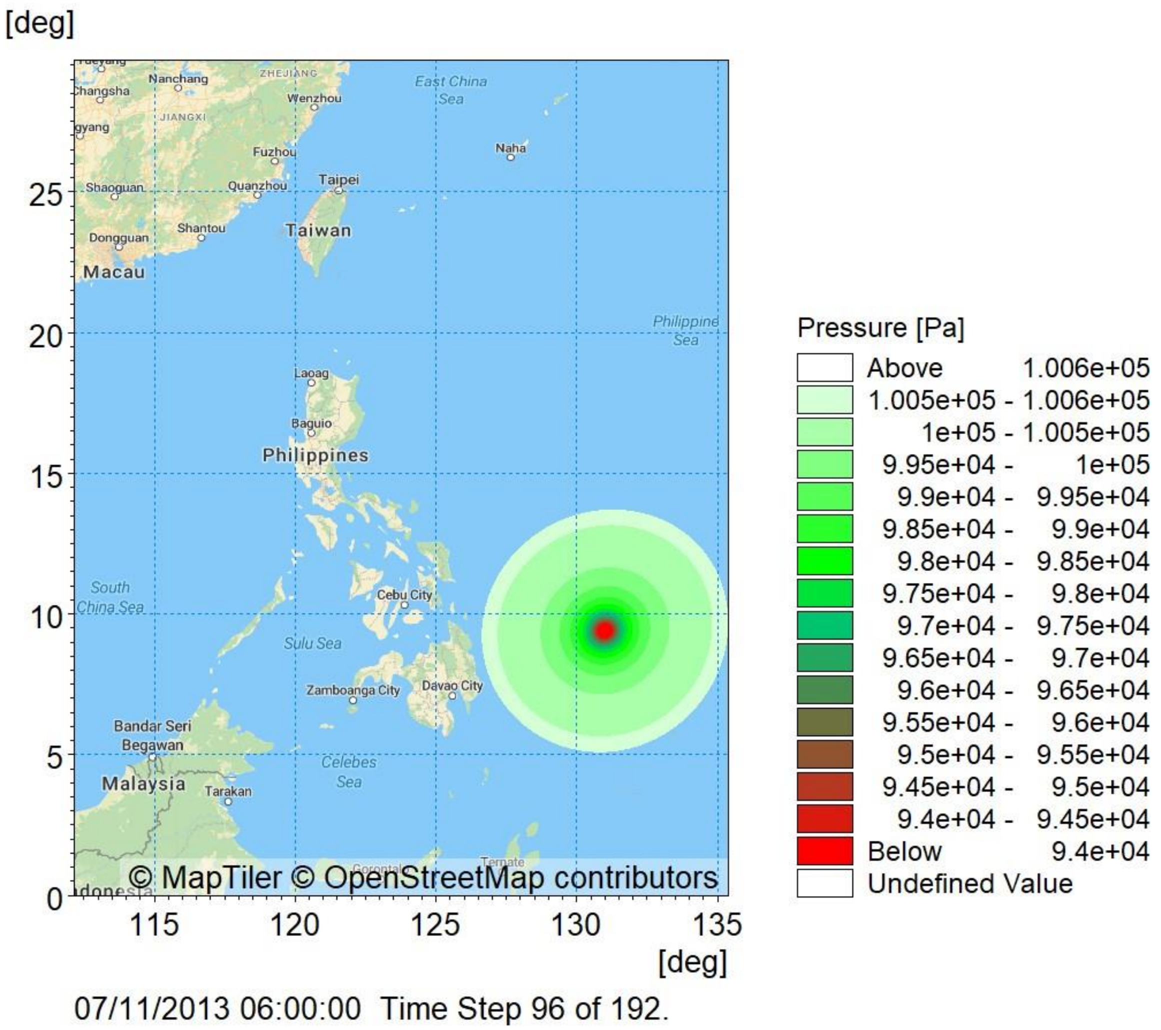

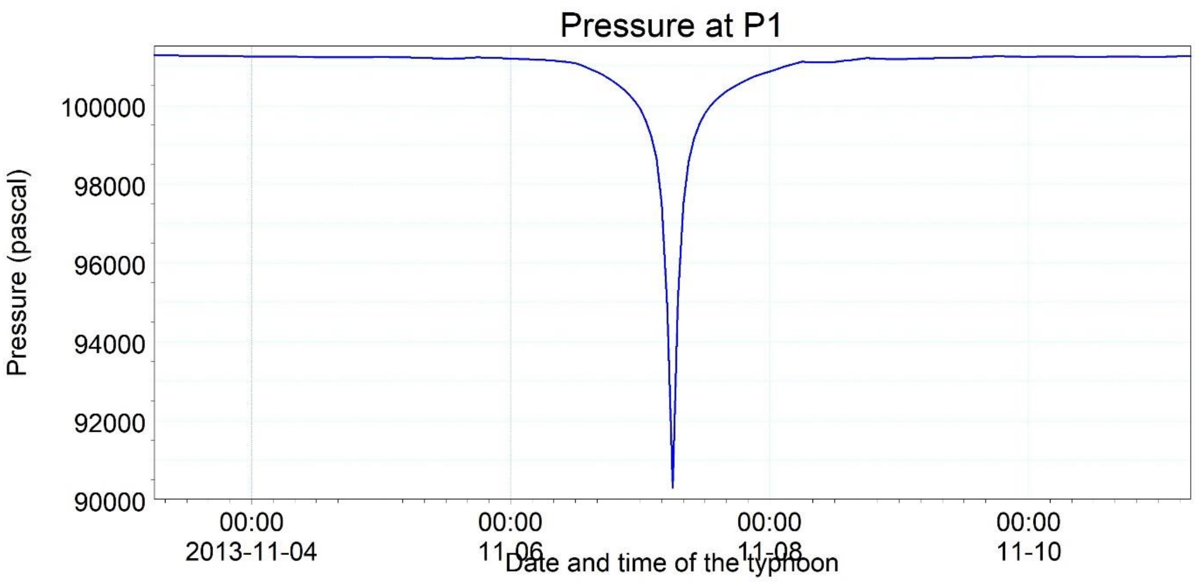

Figure 14: Pressure field of Typhoon Haiyan at P1 (top – 2D pressure field; bottom – time-series of pressure)

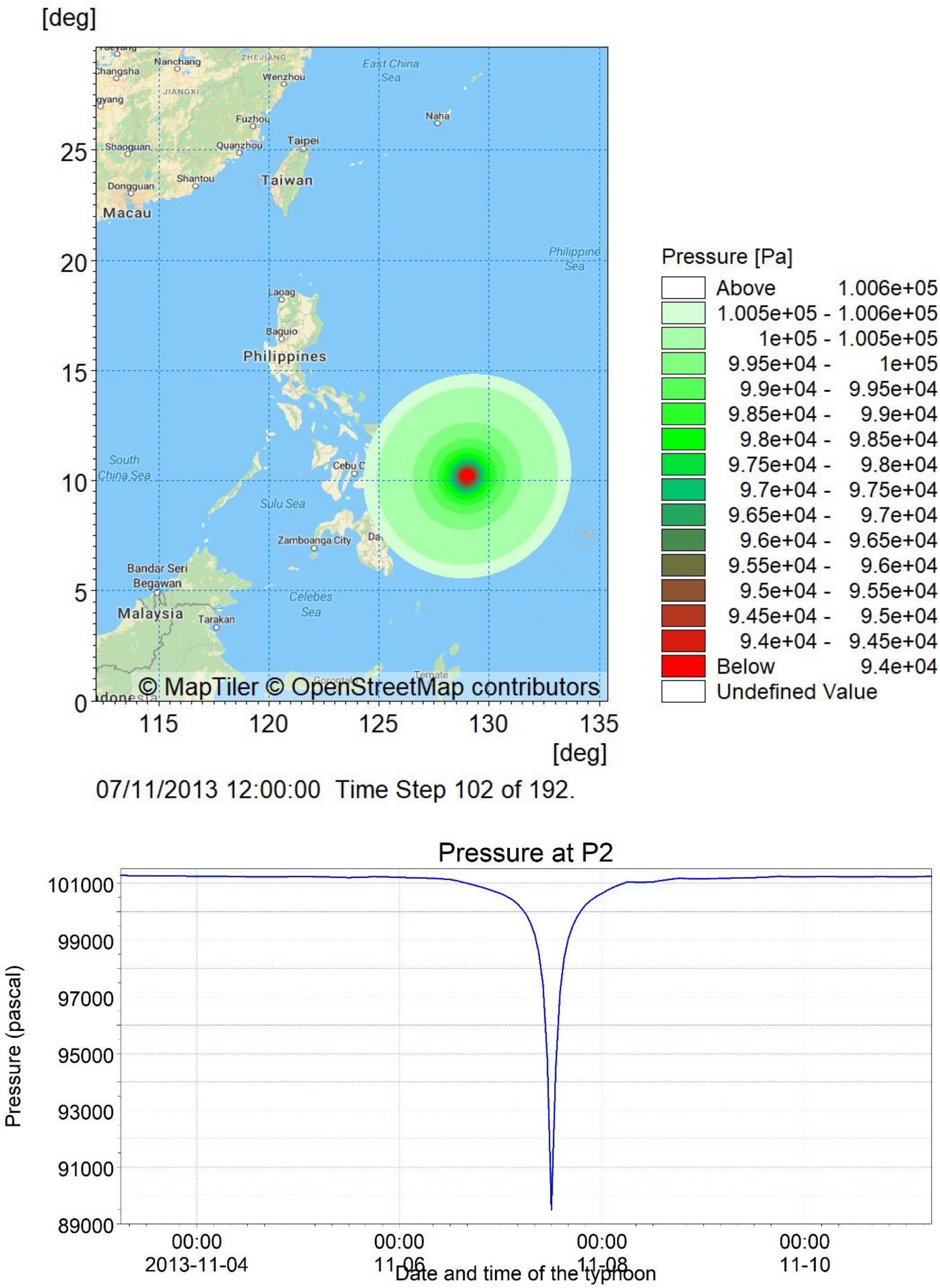

Figure 15: Pressure field of Typhoon Haiyan at P2 (top – 2D pressure field; bottom – time-series of pressure)

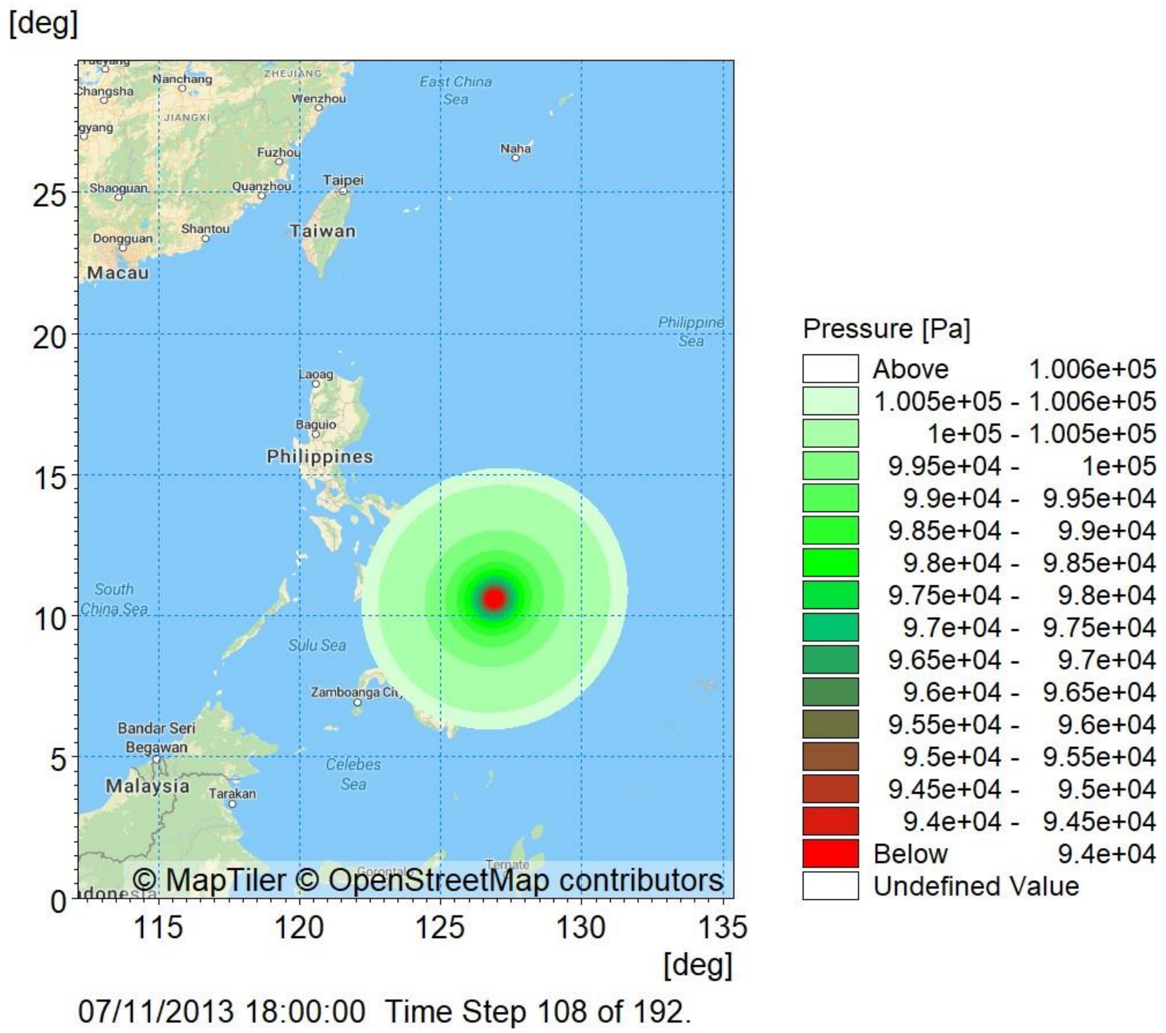

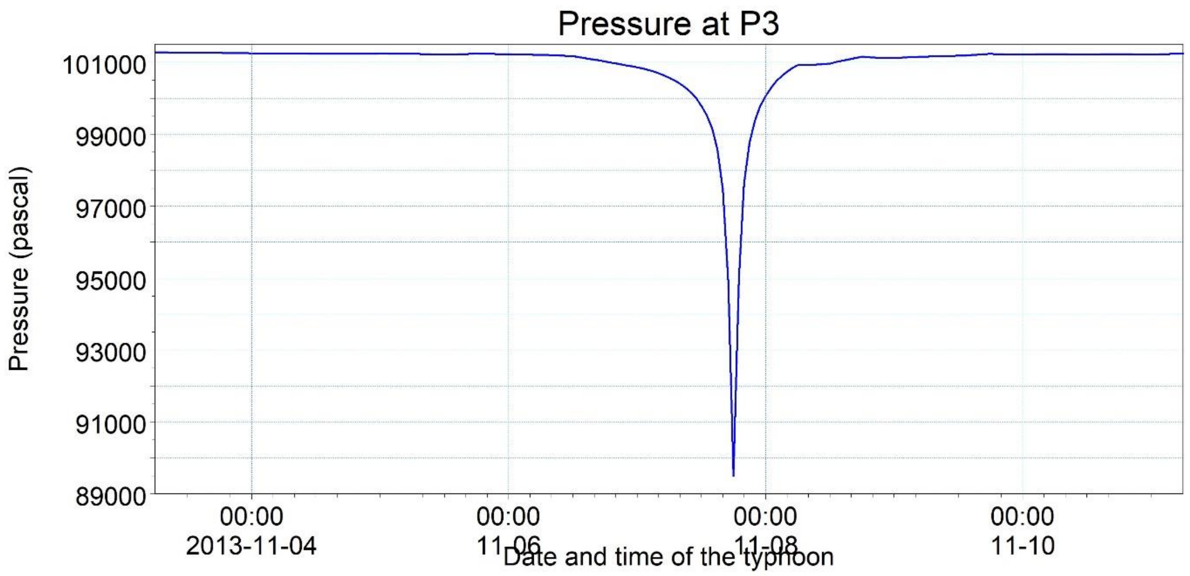

Figure 16: Pressure field of Typhoon Haiyan at P3 (top – 2D pressure field; bottom – time-series of pressure)

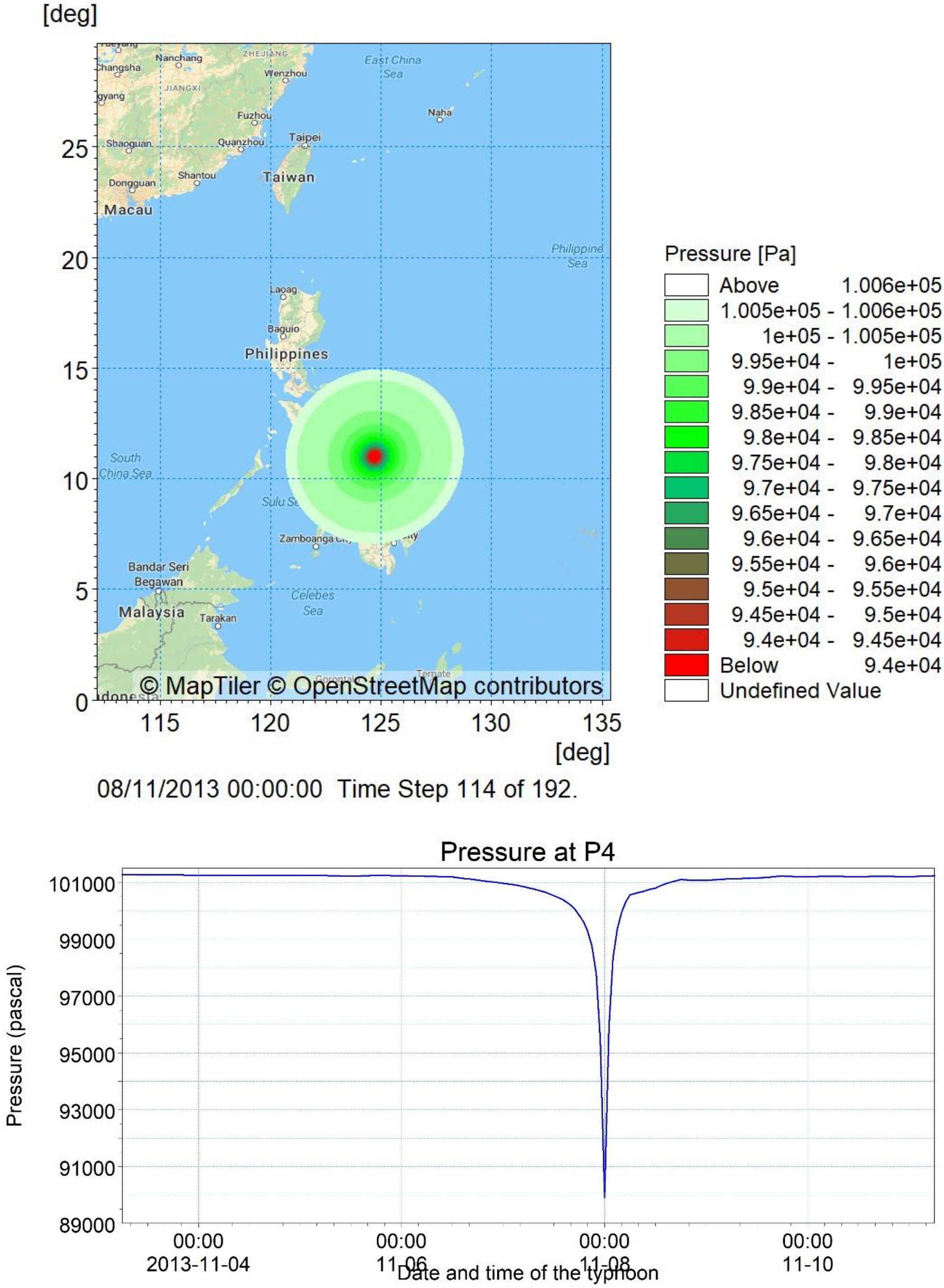

Figure 17: Pressure field of Typhoon Haiyan at P4 (top – 2D pressure field; bottom – time-series of pressure)

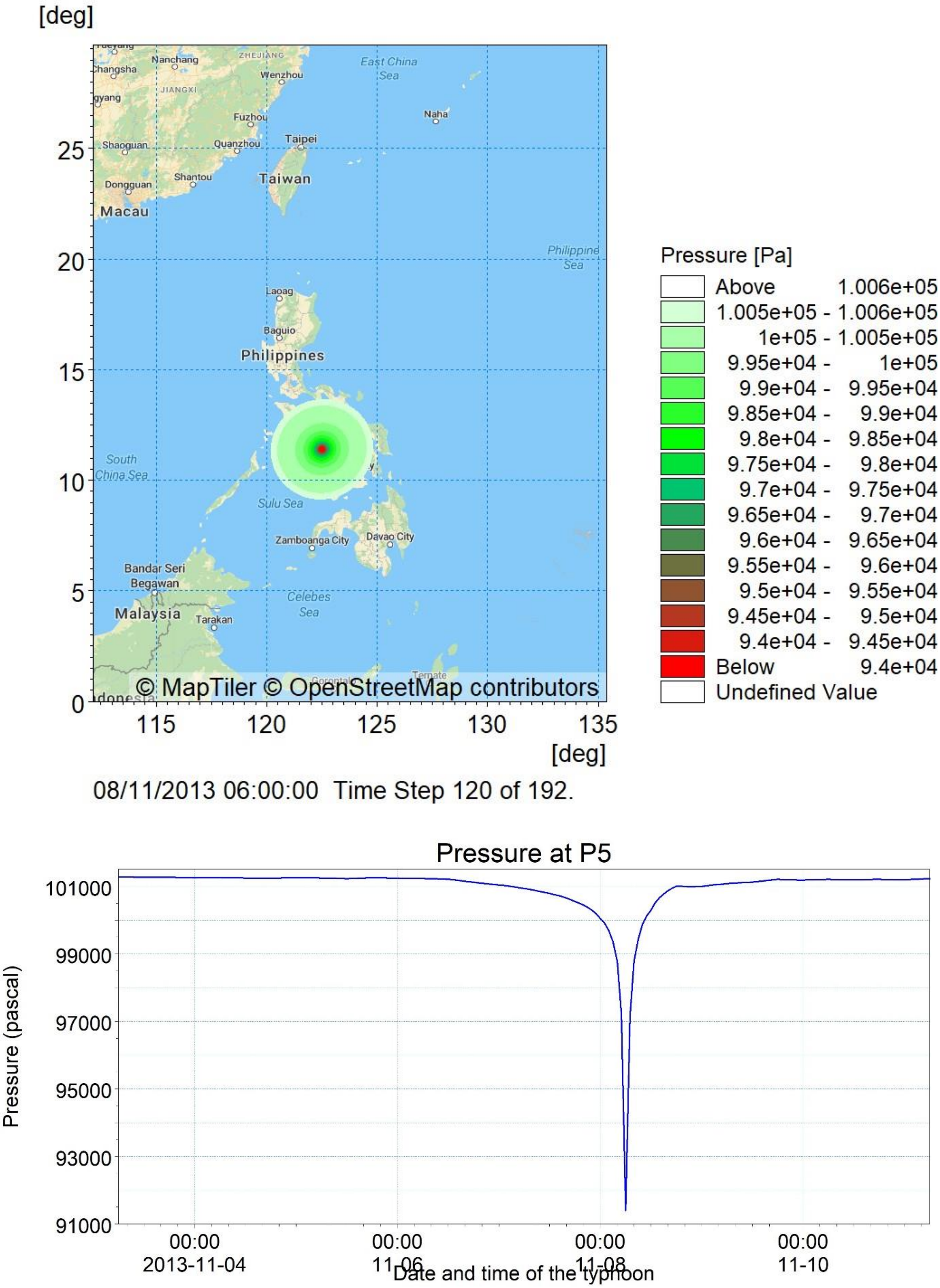

Figure 18: Pressure field of Typhoon Haiyan at P5 (top – 2D pressure field; bottom – time-series of pressure)

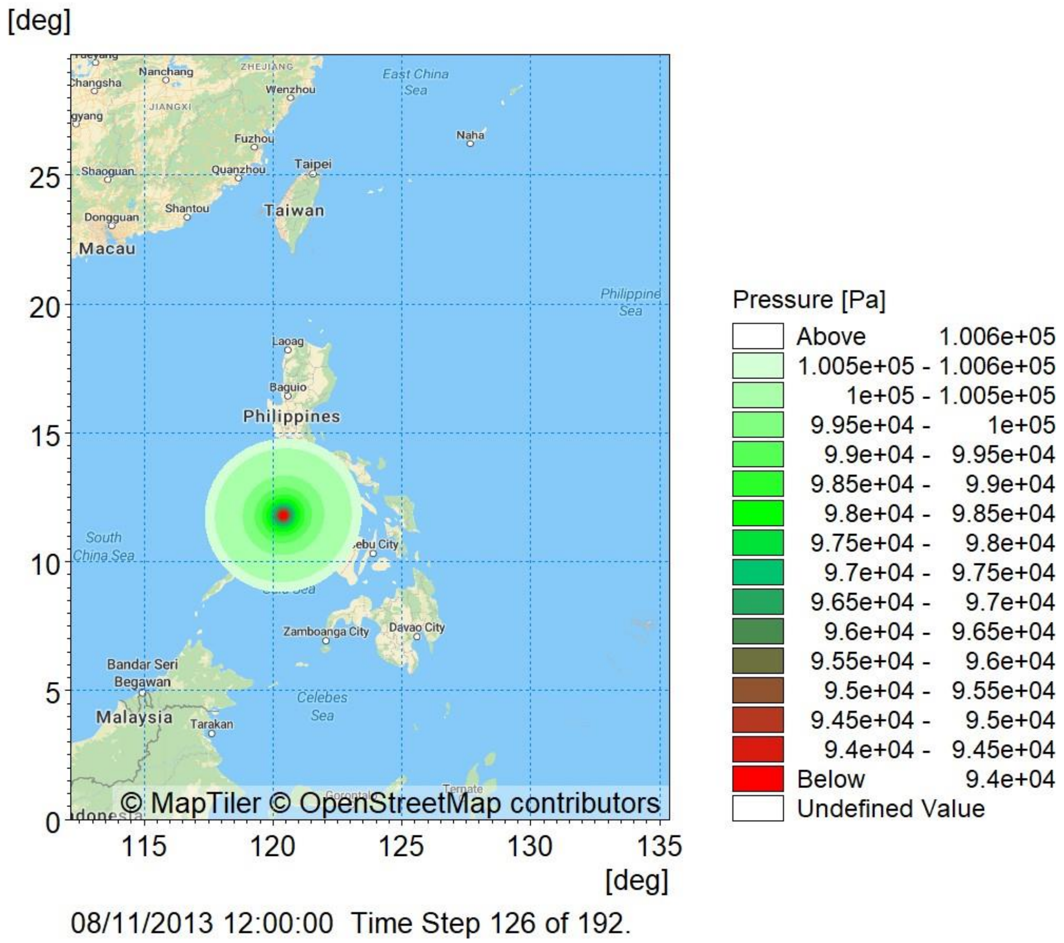

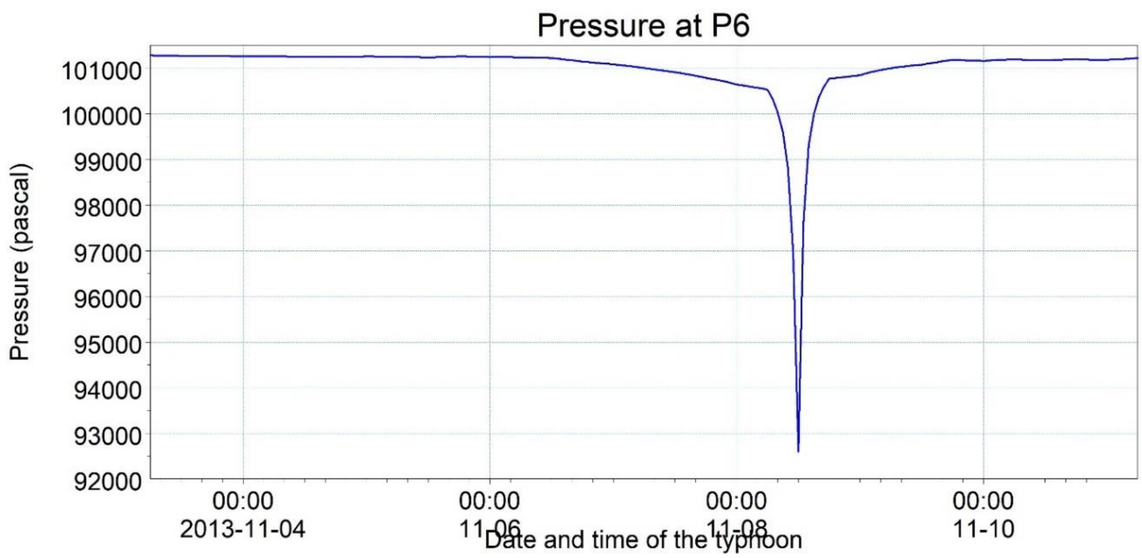

Figure 19: Pressure field of Typhoon Haiyan at P6 (top – 2D pressure field; bottom – time-series of pressure)

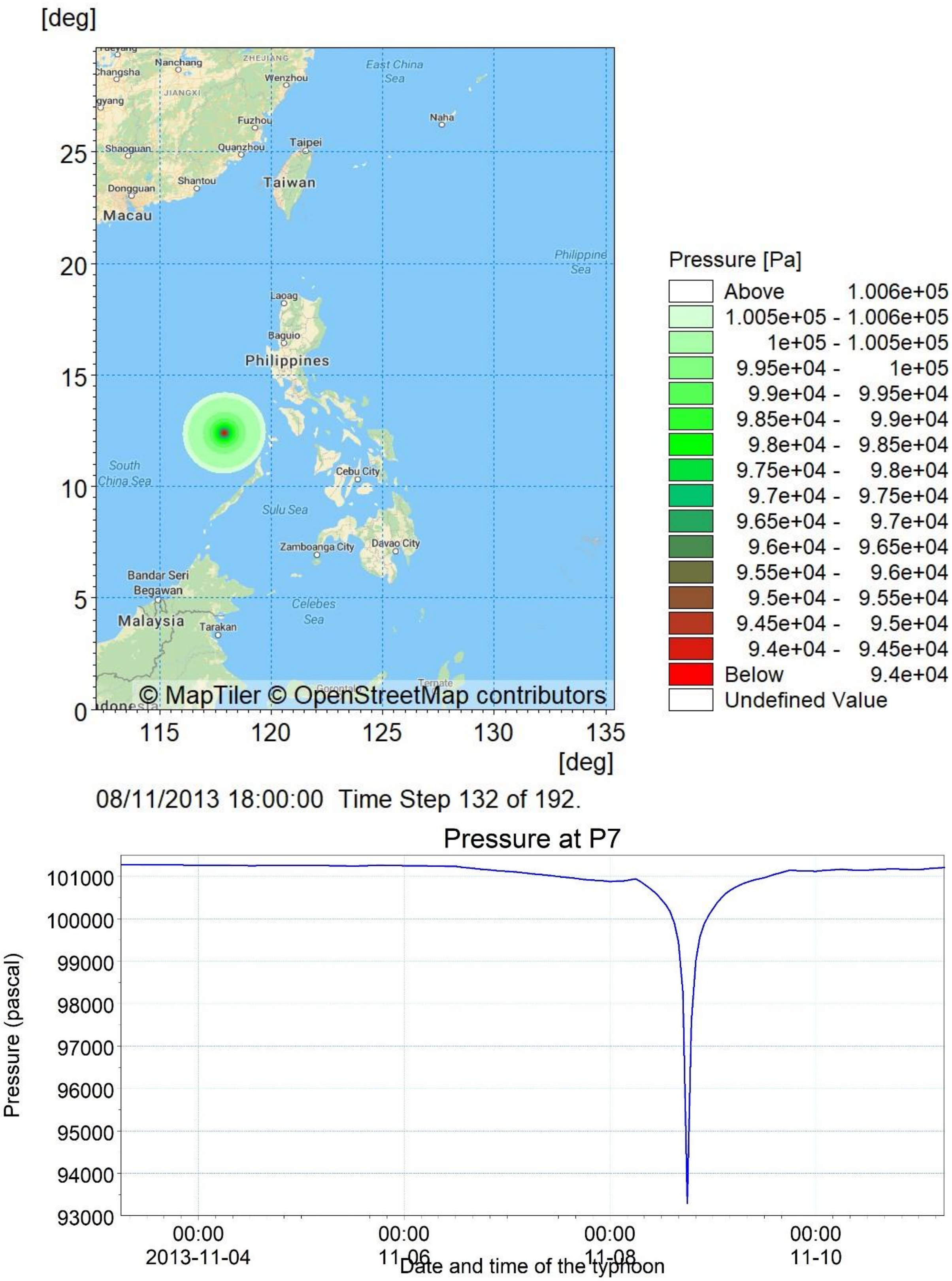

Figure 20: Pressure field of Typhoon Haiyan at P7 (top – 2D pressure field; bottom – time-series of pressure)

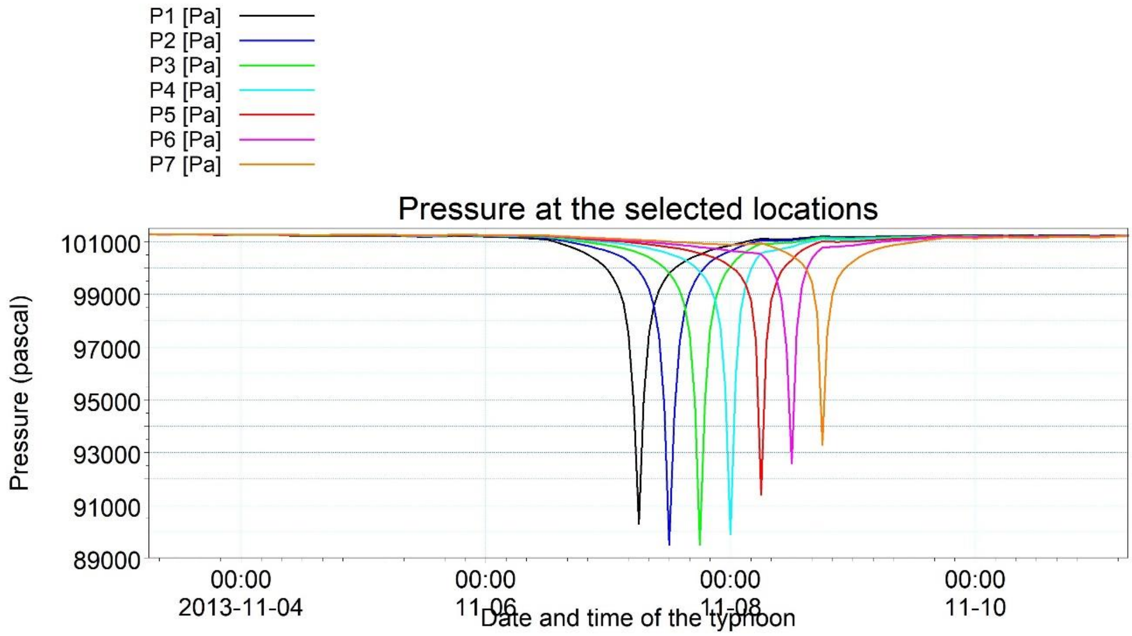

Figure 21: Time-series of pressure at the selected locations during the entire passage of Typhoon Haiyan

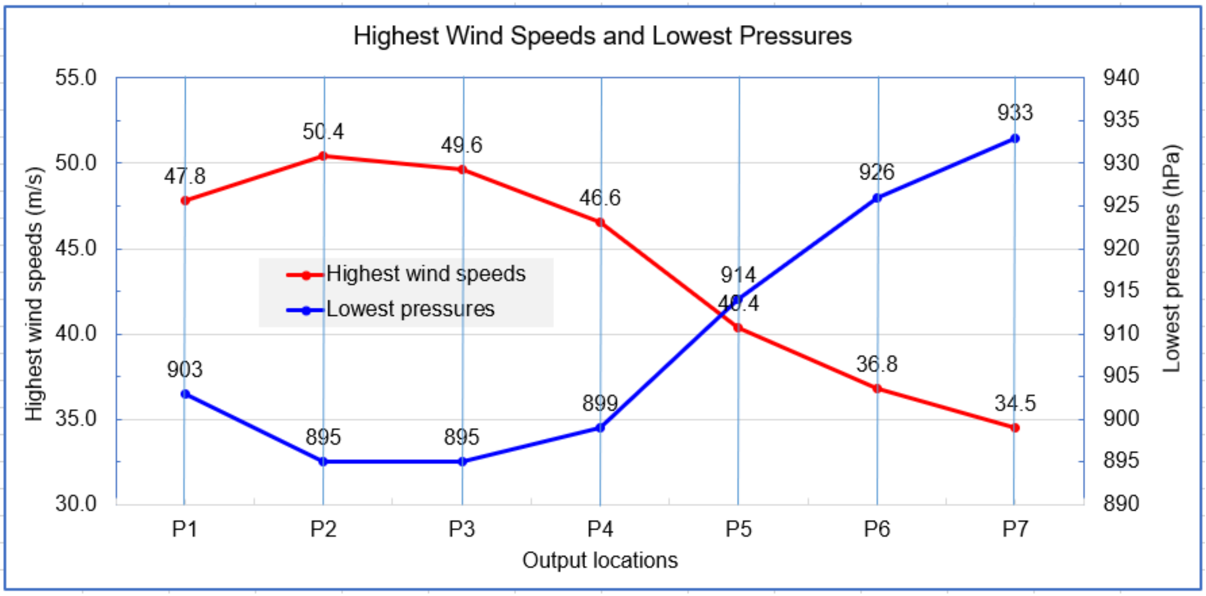

Figure 22: Highest wind speeds and lowest pressures during Typhoon Haiyan at the selected locations extracted from the time-series plots